AD_____

Award Number: DAMD17-99-1-9444

TITLE: Rational Derivatives of Maspin as Candidate Tumor Suppressive Agents of Breast Cancer

PRINCIPAL INVESTIGATOR: Shijie Sheng, Ph.D.

CONTRACTING ORGANIZATION: Wayne State University
Detroit, Michigan 48202

REPORT DATE: August 2002

TYPE OF REPORT: Final

PREPARED FOR: U.S. Army Medical Research and Materiel Command
Fort Detrick, Maryland 21702-5012

# REPORT DOCUMENTATION PAGE

*Form Approved*
*OMB No. 074-0188*



| 1. AGENCY USE ONLY (Leave blank) | 2. REPORT DATE | 3. REPORT TYPE AND DATES COVERED |
|---|---|---|
| | August 2002 | Final (1 Jul 99 - 1 Jul 02) |

**4. TITLE AND SUBTITLE**
Rational Derivatives of Maspin as Candidate Tumor Suppressive Agents of Breast Cancer

**5. FUNDING NUMBERS**
DAMD17-99-1-9444

**6. AUTHOR(S)**
Shijie Sheng, Ph.D.

**7. PERFORMING ORGANIZATION NAME(S) AND ADDRESS(ES)**
Wayne State University
Detroit, Michigan 48202

E-Mail: ae4524@wayne.edu

**8. PERFORMING ORGANIZATION REPORT NUMBER**

**9. SPONSORING / MONITORING AGENCY NAME(S) AND ADDRESS(ES)**
U.S. Army Medical Research and Materiel Command
Fort Detrick, Maryland 21702-5012

**10. SPONSORING / MONITORING AGENCY REPORT NUMBER**

**11. SUPPLEMENTARY NOTES**

**12a. DISTRIBUTION / AVAILABILITY STATEMENT**
Approved for Public Release; Distribution Unlimited

**12b. DISTRIBUTION CODE**

**13. ABSTRACT (Maximum 200 Words)**

See abstract for Part I on page 1, Part II on page 14, and Part III on page 28.

**14. SUBJECT TERMS**
Breast Cancer

**15. NUMBER OF PAGES**
41

**16. PRICE CODE**

| 17. SECURITY CLASSIFICATION OF REPORT | 18. SECURITY CLASSIFICATION OF THIS PAGE | 19. SECURITY CLASSIFICATION OF ABSTRACT | 20. LIMITATION OF ABSTRACT |
|---|---|---|---|
| Unclassified | Unclassified | Unclassified | Unlimited |

Table of Contents

# FINAL REPORT

We proposed to generate and characterize rational derivatives of maspin as candidate tumor suppressive agents of breast cancer. We plan to produce these novel maspin variants as purified proteins (**Specific Objective 1**), and as re-expressed proteins in breast tumor cells that are transfected with the corresponding coding cDNAs (**Specific Objective 2**). The biological functions of these maspin derivatives as well as the wild type maspin will be examined using comprehensive cellular and biochemical assays that have been established in my laboratory. In particular, we planed to focus on the effect of these molecules on tumor growth, cell adhesion, cell motility and invasion. In addition the biochemical and biophysical properties of these new molecules will be evaluated.

PART I

## MASPIN SENSITIZES BREAST CARCINOMA CELLS TO INDUCED APOPTOSIS

Ning Jiang, Yonghong Meng, Suliang Zhang, Edith Mensah-Osman, and Shijie Sheng
Oncogene 2002

ABSTRACT
Maspin, a novel serine protease inhibitor (serpin), suppresses the growth and metastasis of breast tumor *in vivo*. However, the underlying molecular mechanism is unclear. In the current study, we report the first evidence that endogenous maspin expression in mammary carcinoma cells MDA-MB-435 enhanced staurosporine (STS)-induced apoptosis as judged by the increased fragmentation of DNA, increased proteolytic inactivation of poly-[ADP-ribose]-polymerase (PARP), as well as the increased activation of caspase-8 and caspase-3. In parallel, recombinant maspin did not directly regulate the proteolytic activities of either caspase-3 or caspase-8 *in vitro*. Consistent with this result, maspin expressing normal mammary epithelial cells underwent more rapid STS-induced apoptosis as compared to breast carcinoma cells. Interestingly, maspin transfectant cells did not undergo spontaneous apoptosis in the absence of STS. Moreover, neither purified maspin protein added from outside nor endogenous maspin secreted to the cell culture media sensitized cells to STS-induced apoptosis. To investigate the structural determinants of maspin in its apoptosis-sensitizing effect, MDA-MB-435 cells were also transfected with maspin/PAI-1 and PAI-1/maspin chimeric constructs resulting from swapping the N-terminal and the C-terminal domains between maspin and PAI-1 (plasminogen activator inhibitor type 1). The resulting stable transfectant clones expressing maspin/PAI-1 and PAI-1/maspin, respectively, did not undergo spontaneous apoptosis, and were similarly inhibited as maspin transfectant cells in motility assay. Interestingly, however, expression of both maspin/PAI-1 and PAI-1/maspin in MDA-MB-435 cells failed to sensitize these cells to STS-induced apoptosis. Taken together, our evidence provides new insights into the complex molecular mechanisms of maspin that may suppress breast tumor progression not only at the step of invasion and motility, but also by regulating tumor cell apoptosis. The sensitizing effect of maspin on apoptosis is to be contrasted by the pro-survival effect of several other serpins.

## INTRODUCTION

Since the identification of the maspin gene (mammary serine protease inhibitor) based on its expression in normal but not in tumor-derived human mammary epithelial cells (Zou Z, 1994), accumulated functional evidence demonstrates that maspin suppresses tumor metastasis, in part, by inhibiting tumor cell invasion and motility (Sheng S, 1996; Sheng S, 1994; Zhang M, 1997; Zou Z, 1994). Maspin protein has a sequence homology with many serpins including plasminogen activator

inhibitor-type 1, and -type 2 (PAI-1 and PAI-2). Recent *in vitro* evidence that maspin inhibits fibrinogen-associated tissue-type plasminogen activator (tPA) (Sheng, 1998) and prostate tumor cell surface-associated urokinase plasminogen activator (uPA) (Biliran H Jr, 2001; McGowen, 2000) led to a working hypothesis that maspin inhibits tumor invasion and metastasis by blocking the pericellular plasminogen activation cascade.

Meanwhile, emerging evidence also suggests that the anti-metastasis function of maspin may not be limited to the steps of tumor cell invasion and migration. As compared to the parental mammary carcinoma cells MDA-MB-435 or the mock control cells, stable maspin-expressing transfectant clones produced tumors of significantly reduced sizes at the orthotopic implantation sites in nude mice (Sager R, 1996; Zou Z, 1994). Zhang et al subsequently reported that maspin transgene expression in mouse mammary gland inhibited Simian Virus 40 (SV40) large T-antigen induced breast carcinogenesis, and correlated with increased programmed cell death, or apoptosis (Zhang M, 2000). Independent *in vitro* study of Li, et al showed that apoptosis induced by manganese-containing superoxide dismutase was associated with elevated maspin expression level (Li JJ, 1998). These results led to the speculation that maspin may also play a role in apoptosis. It is important to bear in mind, however, that normal mammary epithelial cells that express high level of maspin do not undergo detectable apoptosis either *in vivo* or *in vitro*. Moreover, maspin neither alters the growth kinetics of a variety of breast epithelial cell lines, nor directly induces apoptosis *in vitro* (Shao ZM, 1998; Sheng S, 1996; Sheng S, 1994). Thus, the maspin effect on apoptosis may be a part of cellular response to specific pathological or pharmacological apoptotic stimuli.

In this report, we showed that maspin re-expression in breast carcinoma cells is not sufficient to induce apoptosis *in vitro*. However, it sensitizes cells to staurosporine (STS)-induced apoptosis, which is mediated, at least in part, by the caspase-8/caspase-3 pathway. Interestingly, maspin reactive site loop (RSL) sequence that has been shown to play a critical role in the maspin effect on tumor cell invasion/motility and on plasminogen activation (Biliran H Jr, 2001; McGowen, 2000; Sheng S, 1996; Sheng S, 1994; Sheng, 1998) appeared to be essential but not sufficient for the maspin effect in sensitizing cells to induced apoptosis. Taken together, our data suggests that maspin may regulate tumor cell apoptosis by a distinct mechanism. This study provides exciting new insights into the functional complexity, and the potential application of tumor suppressive maspin for enhancing the efficacy of chemotherapeutic agents.

## RESULTS

### Maspin Sensitizes MDA-MB-435 Cells to Staurosporine-induced Apoptosis.

Maspin has been shown to inhibit tumor cell invasion and motility (Seftor et al., 1998; Sheng S, 1996; Zhang M, 1997; Zou Z, 1994). The evidence that maspin expression correlates with increased sensitivity of mammary epithelial cells to apoptosis (Li JJ, 1998; Shao ZM, 1998; Zhang M, 2000; Zhang et al., 1999) raised the possibility that the maspin effect on tumor cell motility/invasion may result from an increased cell apoptosis. To address this possibility, stable maspin transfectant clones derived from mammary carcinoma cells MDA-MB-435, Tn15 and Tn16, along with a mock transfectant clone pCIneo were first examined in parallel by motility assay and by caspase-3 activity assay. The motility of Tn15 and Tn16 was inhibited by at least 7-fold compared to parental MDA-MB-435 and the pCIneo control clone (Figure 1A). This result was in good agreement with an earlier report (Sheng S, 1996). Under the same culture condition, all cell lines tested were not apoptotic and exhibited similar negligible level of caspase-3 activities (Figure 1B).

To test whether maspin plays a role in induced apoptosis, staurosporine (STS), a strong protein kinase C inhibitor and a well-studied apoptosis inducer (Gomez-Angelats M, 2000; Jacobsen MD, 1996;

Tamaoki T, 1986; Tang D, 2000), was used to induce apoptosis. The apoptotic effect of STS was first evaluated by a modified TdT-mediated dUTP Nick-End Labeling (TUNEL) assay. When the mock control cells were treated with STS in the range of 0.5 to 2 μM for 24 hours, a dose-dependent apoptosis was observed. In all subsequent experiments, cells were treated with 0.5 μM STS, a minimum concentration to induce detectable DNA fragmentation in the pCIneo cells. As shown in Figure 2, after the treatment for 24 hours, the pCIneo cells showed significant shrinkage that is typical for STS-induced apoptosis (Gomez-Angelats M, 2000; Jacobsen MD, 1996; Tang D, 2000). However, only a small fraction ($10 \pm 2.4\%$) of this cell population gave rise to a detectable TUNEL reactivity. In parallel, STS treatment of maspin-expressing transfectant clone Tn15 led to not only cell shrinkage, but also a high level of DNA fragmentation in $54 \pm 5.5\%$ of the total cell population. STS treated Tn16 and three other maspin transfectant clones exhibited a TUNEL reactivity comparable to that of STS treated Tn15 (data not shown). Interestingly, normal mammary epithelial cells 70N that express maspin at a high level (Zou Z, 1994) were even more sensitive to STS-induced apoptosis than Tn15 (and Tn16) cells. In fact, treatment of 70N cells with 0.5 μM STS for 24 hours lead to complete cell detachment and death (data not shown). When treated with 0.5 μM STS for 12 hours, 70N cells remained largely adherent, but showed a high level of DNA fragmentation, comparable to that found in STS-treated Tn15 cells (for 24 hours).

To verify the differential DNA fragmentation patterns among different cell lines at the molecular level, total DNA was isolated from pCIneo cells and maspin transfectant clones. As shown in Figure 3A, little or no DNA fragmentation was detected in all untreated cell lines. STS treatment led to marginal DNA fragmentation in pCIneo cells. In contrast, STS-treated Tn15 (and Tn16, data not shown) and 70N cells gave rise to fragmented DNA at a significantly elevated level. Western blot analysis showed (Figure 3B) that pCIneo cells, both untreated and STS-treated, expressed no detectable maspin. On the other hand, the constitutively expressed maspin in transfectant clones was not altered by STS-induced apoptosis.

A hallmark of cellular response to apoptotic DNA fragmentation is the inactivation of poly-[ADP-ribose]-polymerase (PARP), an enzyme that catalyzes nuclear protein ribosylation and facilitates DNA damage repair (Bromme HJ, 1996). The inactivation of the 116 kDa PARP is carried out by specific proteolytic cleavage, yielding an 85 kDa PARP fragment (Boulares AH, 1999; D'Amours D, 1998). As shown in Figure 3B, the conversion of PARP from 116 kDa to 85 kDa was significantly increased in Tn15 and Tn16 cells as compared to that in pCIneo cells. This data further confirms that maspin expression indeed sensitized cells to STS-induced cell death via an apoptotic mechanism. Taken together, endogenous maspin expression was not sufficient to cause spontaneous cell death. However, it sensitized MDA-MB-435 cells to STS-induced apoptosis.

**The Maspin Effect on STS-induced Caspase-8/Caspase-3 Activation.**

Accumulated evidence supports that the proteolytic fragmentation of PARP is a down-stream event of the activation of caspase-3 (Boulares AH, 1999; D'Amours D, 1998). The caspase-3 activity in pCIneo cells started to increase 30 minutes after the STS-treatments and reached maximum activity after 7 to 8 hours. In parallel, maspin transfectant clones exhibited a greatly enhanced activation of caspase-3. As shown in Figure 4A, 4 hours after the STS treatment, the caspase-3 activity in Tn15 and Tn16 was at least 5-fold higher than that in pCIneo cells. This response was repeatedly shown in three other maspin transfectant clones (data not shown).

Caspase-3 is a cysteine protease. To test whether maspin protein directly regulates the activity of caspase-3, purified recombinant rMaspin was added up to 200 nM to the caspase-3 activity assay mixtures containing the lysate of pCIneo (or MDA-MB-435, data not shown). As shown in Figure 4B, rMaspin did not have any significant effect on either the basal level or the STS-induced caspase-3

activity. Thus, it is unlikely that maspin directly stimulated caspase-3 activity. On the other hand, since neither the level nor the integrity of the constitutively expressed maspin in transfectant clones was altered by STS-induced apoptosis (Figure 3B), it is also unlikely that maspin acted as a substrate of caspase-3 or other intracellular proteolytic enzymes.

It is thought that caspase-3 can be proteolytically cleaved and activated by caspase-8 (Budihardjo I, 1999). To test whether maspin sensitized-apoptosis involved this specific caspase activation pathway, caspase-8 activity in cell lysates were analyzed using a caspase-8 specific fluorogenic substrate. As shown in Figure 4C, pCIneo cells exhibited an increase of caspase-8 activity as soon as 2 hours after the STS-treatment. As compared to pCIneo cells, maspin transfectant cells underwent a significantly faster caspase-8 activation (Figure 4C). Thus, maspin appears to facilitate an upstream event that leads to caspase-8/caspase-3 activation.

**Extracellular Maspin Is Not Essential for Sensitizing Cells to STS-induced Apoptosis.** Maspin expressed in Tn15 and Tn16 cells was also detected in the conditioned culture media (CM, Figure 5A). Moreover, previous functional studies suggest that pericellular maspin was active in inhibiting tumor cell motility and invasion (Seftor et al., 1998; Sheng S, 1996). To test whether secreted maspin was responsible for sensitizing STS-induced apoptosis, pCIneo cells were treated by STS in the presence of the CM of either maspin transfectants or pCIneo cells. As shown in Figure 5B, the STS-induced apoptosis as measured by caspase-3 activity (as well as caspase-8 activity, data not shown) was not significantly affected in each case. In parallel, parental MDA-MB-435 cells were treated with STS in the presence or absence of purified recombinant rMaspin at a final concentration of 200 nM. As shown in Figure 5C, rMaspin neither induced apoptosis by itself, nor affected the STS-induced apoptosis. Thus, it is likely that intracellular or cell-associated, rather than extracellular soluble, maspin sensitized cells to STS-induced apoptosis.

**Both the N-terminal Domain and the Novel RSL Sequence of Maspin Are Required to Sensitize STS-induced Apoptosis.**

Maspin has an overall homology with many inhibitory serpins (Zou Z, 1994). However, maspin reactive site loop (RSL) sequence is somewhat deviant from that of the bona fide inhibitory serpins such as PAI-1 and PAI-2 (Lawrence, 1997; Travis J, 1990). In an attempt to investigate the sequence determinants in maspin responsible for sensitizing cells to induced apoptosis, two chimeras named as maspin/PAI-1 and PAI-1/maspin, were constructed using the scheme as illustrated in Figure 6A. In PAI-1/maspin construct, maspin RSL (amino acids 331-346) plus 30 downstream amino acids at its C-terminus was replaced by the corresponding sequence of PAI-1 (amino acids 356-402). In maspin/PAI-1 construct, the maspin N-terminus containing 330 amino acids was replaced by the first 355 amino acids of PAI-1. The sequence of the first 330 amino acids of maspin is 36% homologues with the corresponding fragment of PAI-1. Maspin RSL and PAI-1 RSL (amino acids 356-374) bear 0% homology. The C-terminal 28 amino acids of PAI-1 (down-stream of its RSL) have a sequence 67% identical to the corresponding fragment of maspin (Zou Z, 1994).

Multiple stable maspin/PAI-1 and PAI-1/maspin transfectant clones derived from MDA-MB435 cells, respectively, were selected based initially on their resistance to G418. RT-PCR using the chimera-specific primers confirmed the expression of maspin/PAI-1 (Figure 6Ba) and PAI-1/maspin (Figure 6Ca) at the mRNA level. Western blotting using a maspin-specific antibody detected a 42kDa protein in the cell lysates of all the maspin/PAI-1 transfectant clones tested, but not in the mock control cells (Figure 6Bc). The chimeric PAI-1/maspin protein could not be detected by any maspin-specific antibodies that were available (data not shown), but was detected in the transfectant clones but not in the mock clones by a monoclonal antibody against PAI-1 (Figure 6Cb). The detected PAI-1/maspin protein was slightly smaller than wild type PAI-1.

It has been shown that the inhibitory activity of maspin on cell motility is consistent with its inhibitory effect on cell surface-associated uPA (Biliran H Jr, 2001; McGowen, 2000). Since PAI-1 also inhibits cell surface-associated uPA and cell motility (for review see (Andreasen PA, 2000; Blasi, 1999)), the chimeras resulting from the domain-specific swapping between the N-terminal and the C-terminal domains of maspin and PAI-1 are likely to act as protease inhibitors and be able to block cell migration. Indeed, as shown in Figure 7A, maspin/PAI-1 and PAI-1/maspin transfectant cells were significantly inhibited in cell migration assay, both to a similar extent as maspin transfectant cells (approximately 60-80%). However, when multiple maspin/PAI-1 and PAI-1/maspin clones were treated with STS and subsequently analyzed by TUNEL assay, all these transfectant clones showed a significantly reduced sensitivity towards STS-induced apoptosis as compared to maspin transfectant cells. In fact, both maspin/PAI-1 and PAI-1/maspin clones behaved similarly as the mock control cells (Figure 2). Results obtained from parallel DNA-ladder experiment (Figure 3A) and caspase-3 activity assay (Figure 7B) further showed that maspin/PAI-1 and PAI-1/maspin transfectant clones were neither inhibited, nor further stimulated in STS-induced apoptosis. This data suggests that although the role of maspin in inhibiting pericellular proteolysis and cell motility may be redundant to that of an inhibitory serpin such as PAI-1, the unique apoptosis-sensitizing effect of maspin appears to depend on the integrity of its entire sequence and, thus, its overall conformation.

**DISCUSSION**

The purpose of the current study is to investigate the role of maspin in mammary tumor cell apoptosis. We showed that maspin alone was not sufficient to induce apoptosis. However, we showed for the first time that maspin greatly sensitized breast carcinoma cells MDA-MB-435 to STS-induced apoptosis. Furthermore, the apoptosis-sensitizing effect of maspin appears to depend on its overall sequence. These data not only help explain the earlier observation that overexpression of maspin correlates with increased apoptosis under certain conditions (Li JJ, 1998; Shao ZM, 1998; Zhang M, 2000; Zhang et al., 1999), but also provide exciting new leads regarding the complex tumor suppressive modes of maspin action.

Considering the evidence that maspin is abundantly expressed in normal mammary epithelial cells (Zou Z, 1994) and that maspin expression is increased at several non-apoptotic stages of mammary gland development in a murine model, i.e., puberty, pregnancy and lactation (Zhang M, 1997), it was not surprising that maspin re-expression in MDA-MB-435 cells alone did not cause spontaneous cell death in culture. On the other hand, since several other serpins implicated in apoptosis primarily regulate induced-apoptosis (Dickinson JL, 1995; Kanamori H, 2000; Kwaan HC, 2000; Schleef RR, 2000), the negligible effect of maspin on the growth and survival of MDA-MB-435 cells in maintenance culture (Sheng S, 1996) may be a manifestation in an environment that lacks appropriate apoptotic stimuli. Indeed, as shown in this study, an apoptosis-sensitizing effect of maspin was only evident when cells underwent STS-induced apoptosis.

STS is a strong inhibitor of protein kinase C (PKC) and has been shown to induce apoptosis (Gomez-Angelats M, 2000; Jacobsen MD, 1996; Tamaoki T, 1986; Tang D, 2000), at least in some breast tumor cells, at a step upstream of caspase-8 (Tang D, 2000). This notion is supported by the evidence that protein kinase C protects against cell death mediated by Fas ligand that specifically activates the caspase-8/caspase-3 pathway (Chen CY, 2001). In this study, we showed that endogenous maspin expression further enhanced the STS-induced activation of caspase-8 and caspase-3, proteolytic inactivation of PARP, as well as DNA fragmentation. Consistent with this observation, normal mammary epithelial cells 70N that express a high level of maspin were significantly more sensitive to STS-induced apoptosis as compared to mammary carcinoma cells MDA-MB-435 that do not express

maspin. Taken together, our data suggests that maspin may sensitize STS-induced apoptosis by enhancing the efficiency of the activated apoptosis cascade. While the choice of STS helped simplify the experimental system and address the effect of maspin on a major apoptosis pathway, it has been noted that the role of a serpin in apoptosis may depend on the specific genetic background of the cells as well as the specific apoptotic stimuli. For example, the viral serpin CrmA (cytokine response modifier A) protects cells from induced apoptotic in some cases (Los M, 1995; Miura M, 1995; Miura M, 1993), but occasionally sensitizes cells to induced cell death (Vercammen D, 1998). Thus, it is of key importance for the future study to identify the biological or pathological apoptosis stimuli that are regulated by maspin.

The role of maspin in cell apoptosis may be distinct from that in tumor cell invasion and motility. It has been noted that endogenous maspin is found in cytoplasm, on the cell surface as well as in conditioned culture media (Pemberton et al., 1997; Shao ZM, 1998; Sheng S, 1996). The inhibitory effect of maspin on cell invasion and motility is localized primarily on the cell surface and in pericellular space (Sheng S, 1996; Sheng S, 1994). However, in this study, we found that the addition of maspin-containing conditioned medium or recombinant maspin to pCIneo cells or MDA-MB-435 cells did not have any significant effect on STS-induced apoptosis (Figure 5). This data suggests that extracellular maspin may not be directly involved in regulating induced-apoptosis. Conversely, the intracellular maspin appears to be responsible for its sensitizing effect on induced-apoptosis. This finding is in line with a report that intracellular PAI-2, rather than secreted PAI-2, contributes to the protection of HeLa cells from TNF-α-induced apoptosis in (Dickinson JL, 1998).

Alternatively, in view of the accumulated evidence for a role of uPA and its receptor uPAR in regulating integrin-mediated cell survival (for review see (Ossowski L, 2000)), and our earlier evidence that endogenous expression of maspin led to a dramatic decrease both in cell surface uPA activity and in cell surface-associated uPA and uPAR proteins (Biliran H Jr, 2001), it remains a possibility that maspin may sensitize induced apoptosis by reducing cell surface-associated pro-survival uPA/uPAR complex. In addition, future studies are needed to address whether the biological function of secreted maspin may subsequently feed back the function of intracellular of cell-associated maspin. Vice versa, the maspin effect on induced-apoptosis may eventually reduce the invasive and migratory activity of tumor cells. It is conceivable that intracellular and extracellular maspin co-exist in equilibrium *in vivo*. Furthermore, the biological function of intracellular and extracellular maspin may be delicately balanced by protein trafficking. .

Serpins share a generally conserved sequence and structural framework (Potempa J, 1994). Interestingly, unlike several serpins such as PAI-1 (Kwaan HC, 2000), PAI-2 (Dickinson JL, 1995), PI-9 (Kanamori H, 2000), and PI-10 (Schleef RR, 2000), that have an anti-apoptosis effect, maspin has an apoptosis-sensitizing effect. This maspin effect, therefore, may be dictated by unique elements in its sequence. The current study showed that both maspin/PAI-1 and PAI-1/maspin transfectant clones were significantly inhibited in cell motility (Figure 7) and invasion (data not shown) assays. Since the inhibitory effect of maspin on tumor cell motility and invasion correlates with its inhibitory effect on cell surface-associated uPA (Biliran H Jr, 2001; McGowen, 2000), it is likely that the maspin/PAI-1 and PAI-1/maspin chimeras resulting from swapping the N-terminuses and C-terminuses (containing the RSL sequence) between maspin and the well-characterized anti-proteolytic serpin PAI-1 did not alter the general structural framework that supports the proteolytic inhibitory activity. While more detailed studies are underway to investigate the role of maspin/PAI-1 and PAI-1/maspin on pericellular plasminogen activation, it is of particular importance to note that neither maspin/PAI-1 nor PAI-1/maspin transfectant clones were sensitized to STS-induced apoptosis. Moreover, maspin depended not only on its proteolytic inhibitory potential, but also on the integrity of its overall sequence to sensitize

cells to induced apoptosis. This evidence indicates that the maspin effect on induced apoptosis may not be redundant to that of other serpins such as PAI-1.

To date, the intracellular targets, thus the molecular modes of action, of serpins involved in apoptosis are unknown. The possibility remains that maspin may sensitize induced apoptosis by inhibiting an intracellular protease. To this end, Biswas et al have shown that Go6976, an STS-derived compound that specifically inhibits PKC α- and β- subunits, induces the apoptosis of ER-negative breast carcinoma cells through the inhibition of NF-κB activity (Biswas DK, 2001). Considering the evidence that NF-κB is primarily activated by the ubiquitin-mediated degradation of IκB, a cytosolic inhibitor of NF-κB in its p105 precursor (Lee DH, 1998; Palombella VJ, 1994), it is intriguing to hypothesize that maspin may enhance STS-induced inactivation of NF-κB by blocking the proteolytic degradation of IκB.

On the other hand, considering an earlier evidence that the antiproteolytic activity of PAI-2 was not essential for its anti-apoptotic function (Dickinson JL, 1998), we cannot rule out the possibility that maspin may sensitize cells to induced apoptosis by interacting with an intracellular cognate molecule in a non-inhibitory manner. Based on the novel RSL sequence of maspin, Hopkins and Whisstock speculated that maspin might interact with a thymosin β-4 like molecule that has no proteolytic activity (Hopkins & Whisstock, 1994). While this possibility needs to be further investigated, it is important to note that β-thymosins are a family of small acidic cytoplasmic polypeptides. Beta-4 and β-10 thymosins have been shown to sequester actin and regulate F-actin assembly (Yu FX, 1993). Furthermore, thymosin β-10 has been shown to accelerate TNF-α induced fibroblast apoptosis (Hall, 1995).

In summary, this is the first report that endogenous maspin sensitized cells to induced apoptosis *in vitro*. Together with our earlier evidence, these results suggest that maspin may suppress breast tumor metastasis by two distinct mechanisms: (i) inhibiting tumor cell invasion and motility by neutralizing pericellular proteolytic activities, and (ii) sensitizing tumor cells to induced apoptosis. Extensive studies are underway to evaluate the effect of maspin on induced apoptosis of other types of cells.

## MATERIALS AND METHODS

**Cell Culture and Reagents.** Breast carcinoma cell line MDA-MB-435 was obtained from American Type Culture Collection (Rockville, MD) and maintained in α-MEM (Life Technologies Inc., NY) supplemented with 5% fetal calf serum (FCS) (Hyclone, UT). Stable maspin transfectant clones (Tn 15 and Tn16) and the mock transfectant clone (pCIneo) derived from MDA-MB-435 cells were generated and cultured as described (Sheng S, 1996). Normal mammary epithelial cells 70N were culture in DFCI-1 medium (Band V, 1989). Recombinant maspin was overexpressed in Baculo-virus infected insect cells *Sf*9, and was purified as previously described (Sheng S, 1994). All other chemicals, unless otherwise specified, were obtained from SIGMA (St. Louis, MO) in the highest suitable purities. All oligonucleotides were customer-designed and synthesized by Life Technologies Inc.

**Construction and Endogenous Expression of Maspin/PAI-1 and PAI-1/maspin Chimeras.** For the construction of maspin/PAI-1, a DraIII cloning site was generated by PCR at the position 11 amino acids upstream from the PAI-1 $P_1P_1'$ peptide bond. A 3'-terminal EcoRI cloning site was created down-stream of PAI-1 translation stop codon. The primers used were 5'-GCTGCACAAAGTGAA-GATCGAGGTGAACG-3' and 5'-CCGAATTCAAAGGTCCTCCAAGGAGAGG-3', respectively. The 5'-DraIII to 3'-EcoRI fragment of this C-terminal domain of PAI-1 was then ligated to the N-terminal fragment of maspin cDNA generated by EcoRI/DraIII double digestion of the pBluescript/maspin plasmid cDNA (Zou Z, 1994). DNA sequencing (Pathology Laboratory, WSU) confirmed that the maspin/PAI-1 construct contained 330 N-terminal amino acids of wild type maspin and 47 amino acids of the C-terminal domain of wild type PAI-1. The full-length maspin/PAI-1 coding sequence was

subcloned into a mammalian expression vector pCIneo (Promega, WI) to generate pMaspin/PAI-1 plasmid.

For the construction of PAI-1/maspin, an EcoRI cloning site was engineered immediately upstream of the 5' terminus of wild type PAI-1 cDNA. A DraIII cloning site was generated by PCR at the position 15 amino acids upstream from the PAI-1 $P_1P_1$' peptide bond. The primers used were 5'-CCGAATTCGCAAGGCACCTCTGAGAACT-3' and 5'-CTTCACTTTGTGCAGCGCCTGCGC-3', respectively. The 5'-EcoRI to 3'-DraIII fragment of this N-terminal domain of PAI-1 was then ligated to the C-terminal fragment of maspin cDNA generated by DraIII/XbaI double digestion of the pBluescript/maspin plasmid cDNA (Zou Z, 1994). DNA sequencing (Pathology Laboratory, WSU) confirmed that the maspin/PAI-1 construct encodes 355 N-terminal amino acids of wild type PAI-1 followed by 46 amino acids of the C-terminal domain of wild type maspin. The full length PAI-1/maspin coding sequence was subcloned into a mammalian expression vector pCIneo (Promega, WI) to generate pPAI-1/maspin plasmid.

To express endogenous maspin/PAI-1 and PAI-1/maspin chimeras, MDA-MB-435 cells were transfected with pMaspin/PAI-1, pPAI-1/maspin, and pCIneo vector DNA, respectively, using an electroporation procedure (Sheng S, 1996; Zou Z, 1994). Briefly, approximately 1 x $10^7$ MDA-MB-435 cells harvested in log phase were electroporated with 40 μg of each plasmid DNA at 250V and 960 microfarads in α-MEM containing 5% FCS. The electroporated cells were cultured in 24-well plates in α-MEM supplemented with 5% FCS and 1 mg/ml geneticin (or G418, Life Technologies Inc.) for 14 days. The surviving individual clones were chosen using cloning rings (Bel-Art Products, NJ), and maintained routinely in the presence of 500 μg/ml geneticin. Twenty individual clones were expanded for each transfection reaction.

**Reverse Transcription-PCR.** Total RNA was extracted from cells using the RNeasy Mini Kit (Qiagen). The extracted RNA was reverse-transcribed with the AMV reverse transcriptase (Promega) in the presence of oligo$(dT)_{15}$ primer as described by the manufacturer. The resulting cDNA preparation was subjected to PCR amplification using template-specific upstream and downstream primers for 25 cycles. Each PCR cycle included a denaturation step at 94 °C for 30 seconds; a primer-annealing step at 55 °C for 45 seconds (maspin, or maspin/PAI-1, or PAI-1/maspin), or at 62 °C for 1 min (GAPDH); and an extension step at 72 °C for 45 seconds. Reactions were performed in a Genius programmable thermal controller model (Techne Incorporated, Duxford, Cambridge). The primers used for PCR amplification of maspin/PAI-1 were 5'-GCGAATTCGGCTTTTGCCGTTGATCTGT-3' and 5'-CCGAATTCGAAG-GTCCTCCAAGGAGAGG-3'. The expected PCR product is about 1200 base pairs of size. The primers sued for PCR amplification of PAI-1/maspin were 5'-CCGAATTCGCAAGGCACCTCTGAGAACT-3' and 5'-CTTCATGAAGCCTGTGGACTCATCCTC-3'. The primers used for GADPH PCR amplification were 5'-ACGGATTTGGTCGTATTGGG-3' and 5'-TGATTTTGGAGGGATCTCGC-3'. The PCR products were analyzed by electrophoresis on 1% agarose gel containing ethidium bromide, and photographed under UV light.

**Western Blotting.** For western blotting of cell lysates, cells were collected using a cell scraper and lysed in a low-salt, protease inhibitor-rich lysis buffer (Sheng S, 1994). A total of 100 μg soluble protein extracted from each transfectant clonal cell line was resolved by 10% SDS-PAGE. For western blotting of conditioned media (CM), CM were collected upon 24 hr incubation of keratinocyte serum free medium (K-SFM) (Life Technologies Inc.), and concentrated approximately 100 fold using Centricon YM-10 concentrators (Millipore, MA). A total of 50 μg soluble protein from each CM sample was applied to 10% SDS-PAGE. Western blotting was performed with monoclonal antibody to maspin (Pharmingen), or monoclonal antibody EGG to PAI-1 (DuPont Merck), or poly(ADP-ribose) polymerase (PARP) (Pharmacia) or β-actin (Pharmacia), and the corresponding horse radish peroxidase-

conjugated secondary antibodies. Immunoreactivity was detected using the enhanced chemiluminescence reagent from Amersham.

**Induced Apoptosis.** Cells cultured in 6-well plates for 24 were incubated with 0.5 μM STS at 37 °C with 6.5 % $CO_2$ for indicated hours. To test the effect of secreted maspin, STS was added to the cells that had been cultured for 24 hours in the K-SFM pre-conditioned (for 24 hours) by maspin transfectants or pCIneo cells. To examine the effect of purified recombinant human maspin (rMaspin) cells were incubated with rMaspin at a final concentration of 20-200 nM for 24 hr prior to the addition of STS.

**TUNEL Assay and Electrophoresis Assays for DNA Fragmentation.**

To detect DNA fragmentation at the cellular level, cells were seeded in 8-well Lab-Tek®II chamber slides at a density of 100,000/well and incubated for 24 hours in the corresponding maintenance media. The cells were treated with 0.5 μM STS 24 hours (with the exception of 12 hours for 70N cells), washed twice with PBS and fixed with freshly prepared 4% paraformaldehyde at room temperature for 25 minutes. The cells were washed and permeabilized in 0.2% Triton X-100 (in PBS) for 5 minutes at room temperature. The cells were then washed and stained by a modified TUNEL procedure using the DeadEnd™ Colorimetric Apoptosis Detection System (Promega, Madison, WI).

To detect DNA fragmentation at the molecular level, cells were seeded in 60 mm petri dishes at a density of 2 x $10^6$/dish and incubated in the corresponding media for 24 hours before the STS treatments. DNA isolated from either STS-treated of untreated cells using the Apoptotic DNA ladder Kit (Roche Diagnostics GmbH, Mannheim, Germany) were analyzed by 1% agarose gel electrophoresis and visualized by ethidium bromide fluorescent staining.

**Caspase Activity Assays.** For caspase-3 activity assay, cells were treated with STS for 4 hr. For caspase-8 activity assay, cells were treated with STS for 2 hr. Following the removal of detached cells by aspirating the culture media, the remaining adherent cells were lysed in 200 μl of 50 mM Tris buffer (pH 7.5) containing 0.05% Nonidet and 1 mM DTT. The clear supernatant (cytosolic fraction) resulting from the centrifugation at 12,000 g for 5 minutes at 4°C was collected. A total of 25 μg protein from each cytosolic fraction was incubated with 40 μM peptide substrate for caspase-3, or caspase-8 for 120 min at 37 °C in 200 μl reaction mixtures containing 10 mM HEPES (pH 7.5), 50 mM NaCl, and 2.5 mM DTT. The peptide substrates for caspase-3 and caspase-8 were Ac-DEVD-AMC and Ac-IETD-AMC, respectively (International Bio, CA). To test the effect of purified maspin on caspase-3 activity, rMaspin was added at 20-200 nM final concentrations along with the fluorogenic substrate of caspase-3 into the assay mixtures. Fluorescence released by caspase activity was measured at 380 $nm_{excitation}$ and 460 $nm_{emission}$ using the SPECTRAmax GEMINI spectrofluorometer (Molecular Devices, CA). The cytosolic fractions of untreated cells were analyzed in parallel and were used as the background.

*In vitro* Motility Assay Using Membrane Invasion Culture System (MICS) was performed as previously described (Sheng S, 1996).

## ACKNOWLEDGEMENTS

This work was supported in part by a Ruth Sager Memorial Fund (to S. S.) and a DOD grant BC0996974 (to S. S.). The authors wish to thank Mr. Hector Biliran, Jr. and Dr. Shuping Yin for critical review and proofreading of the manuscript.

## REFERENCES

Andreasen PA, Egelund R, Petersen HH. (2000). *Cell Mol Life Sci*, **57,** 25-40.
Band V, Sager R. (1989). *Proc Natl Acad Sci U S A*, **86,** 1249-53.
Biliran H Jr, Sheng S. (2001). *Cancer Res*, **61,** 8676-82.

Biswas DK, Dai S, Cruz A, Weiser B, Graner E, Pardee AB. (2001). *Proc Natl Acad Sci U S A*, **98,** 10386-91.
Blasi, F. (1999). *Thromb Haemost*, **82,** 298-304.
Boulares AH, Yakovlev AG, Ivanova V, Stoica BA, Wang G, Iyer S, Smulson M. (1999). *J Biol Chem*, **274**(22932-40.
Bromme HJ, Holtz J. (1996). *Mol Cell Biochem*, **163-164,** 261-75.
Budihardjo I, Oliver H, Lutter M, Luo X, Wang X. (1999). *Annu Rev Cell Dev Biol*, **15,** 269-90.
Chen CY, Juo P, Liou JS, Li CQ, Yu Q, Blenis J, Faller DV. (2001). *Cell Growth Differ*, **12,** 297-306.
D'Amours D, Germain M, Orth K, Dixit VM, Poirier GG. (1998). *Radiat Res*, **150,** 3-10.
Dickinson JL, Bates EJ, Ferrante A, Antalis TM. (1995). *J Biol Chem*, **270,** 27894-904.
Dickinson JL, Norris BJ, Jensen PH, Antalis TM. (1998). *Cell Death Differ*, **5,** 163-71.
Gomez-Angelats M, Bortner CD, Cidlowski JA. (2000). *J Biol Chem*, **275,** 19609-19.
Hall, AK. (1995). *Cell Mol Biol Res*, **41,** 167-80.
Hopkins, P. C. & Whisstock, J. (1994). *Science*, **265,** 1893-4.
Jacobsen MD, Weil M, Raff MC. (1996). *J Cell Biol*, **133,** 1041-51.
Kanamori H, Krieg S, Mao C, Di Pippo VA, Wang S, Zajchowski DA, Shapiro DJ. (2000). *J Biol Chem*, **275,** 5867-73.
Kwaan HC, Wang J, Svoboda K, Declerck PJ. (2000). *Br J Cancer*, **82,** 1702-8.
Lawrence, DA. (1997). *Adv Exp Med Biol*, **425,** 99-108.
Lee DH, Goldberg, AL. (1998). *Trends Cell Biol*, **8,** 397-403.
Li JJ, Colburn NH, Oberley LW. (1998). *Carcinogenesis*, **19,** 833-9.
Los M, Van de Craen M, Penning LC, Schenk H, Westendorp M, Baeuerle PA, Droge W, Krammer PH, Fiers W, Schulze-Osthoff K. (1995). *Nature*, **375,** 81-3.
McGowen, R., Biliran, H. Jr., Sager, R., and Sheng, S. (2000). *Cancer Res.*, **60,** 4771-4778.
Miura M, Friedlander RM, Yuan J. (1995). *Proc Natl Acad Sci U S A*, **92,** 8318-22.
Miura M, Zhu H, Rotello R, Hartwieg EA, Yuan J. (1993). *Cell*, **75,** 653-60.
Ossowski L, Aguirre-Ghiso JA. (2000). *Curr Opin Cell Biol*, **12,** 613-20.
Palombella VJ, Rando OJ, Goldberg AL, Maniatis T. (1994). *Cell*, **78,** 773-85.
Pemberton, P. A., Tipton, A. R., Pavloff, N., Smith, J., Erickson, J. R., Mouchabeck, Z. M. & Kiefer, M. C. (1997). *J Histochem Cytochem*, **45,** 1697-706.
Potempa J, Korzus E, Travis J. (1994). *J Biol Chem*, **269,** 15957-60.
Sager R, Sheng S, Pemberton P, Hendrix MJ. (1996). *Curr Top Microbiol Immunol*, **213,** 51-64.
Schleef RR, Chuang TL. (2000). *J Biol Chem*, **275,** 26385-9.
Seftor, R. E., Seftor, E. A., Sheng, S., Pemberton, P. A., Sager, R. & Hendrix, M. J. (1998). *Cancer Res*, **58,** 5681-5.
Shao ZM, Nguyen M, Alpaugh ML, O'Connell JT, Barsky SH. (1998). *Exp Cell Res*, **241,** 394-403.
Sheng S, Carey J, Seftor EA, Dias L, Hendrix MJ, Sager R. (1996). *Proc Natl Acad Sci U S A*, **93,** 11669-74.
Sheng S, Pemberton PA, Sager R. (1994). *J Biol Chem*, **269,** 30988-93.
Sheng, S., Truong, B., Frederickson, D., Wu, R., Pardee, A. B., and Sager, R. (1998). *Proc. Natl. Acad. Sci. U.S.A.*, **95,** 499-504.
Tamaoki T, Nomoto H, Takahashi I, Kato Y, Morimoto M, Tomita F. (1986). *Biochem Biophys Res Commun*, **135,** 397-402.
Tang D, Lahti JM, Kidd VJ. (2000). *J Biol Chem*, **275,** 9303-7.
Travis J, Guzdek A, Potempa J, Watorek W. (1990). *Biol Chem Hoppe Seyler*, **371,** Suppl:3-11.

Vercammen D, Beyaert R, Denecker G, Goossens V, Van Loo G, Declercq W, Grooten J, Fiers W, Vandenabeele P. (1998). *J Exp Med*, **187,** 1477-85.
Yu FX, Lin SC, Morrison-Bogorad M, Atkinson MA, Yin HL. (1993). *J Biol Chem*, **268,** 502-9.
Zhang M, Sheng S, Maass N, Sager R. (1997). *Mol Med*, **3,** 49-59.
Zhang M, Shi Y, Magit D, Furth PA, Sager R. (2000). *Oncogene*, **19,** 6053-8.
Zhang, M., Magit, D., Botteri, F., Shi, H. Y., He, K., Li, M., Furth, P. & Sager, R. (1999). *Dev Biol*, **215,** 278-87.
Zou Z, Anisowicz A, Hendrix MJ, Thor A, Neveu M, Sheng S, Rafidi K, Seftor E, Sager R. (1994). *Science*, **263,** 526-9.

## FIGURES AND LEGANDS

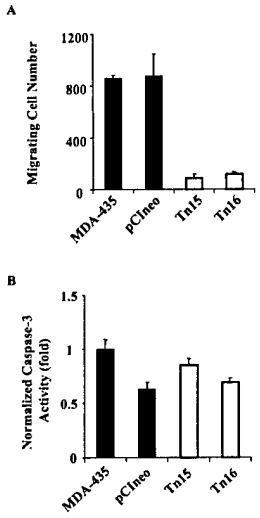


**Figure 1. The Effect of Endogenous Maspin on the Motility and Caspase-3 Activity of Breast Carcinoma MDA-MB-435 Cells. (A)** *In vitro* cell motility assay. Cell motility is presented as the total number of cells that migrated across the matrigel-coated polycarbonate filters. Data represent the average of three parallel experiments and the error bars represent the standard errors. **(B)** Caspase-3 activity assay. Cells were seeded and collected under the same culture condition as in motility assay. The caspase-3 activity (fluorescence unit) in each sample was normalized by caspase-3 activity of parental MDA-MB-435 cells. The data represent the average of three parallel experiments and the error bars represent the standard errors.

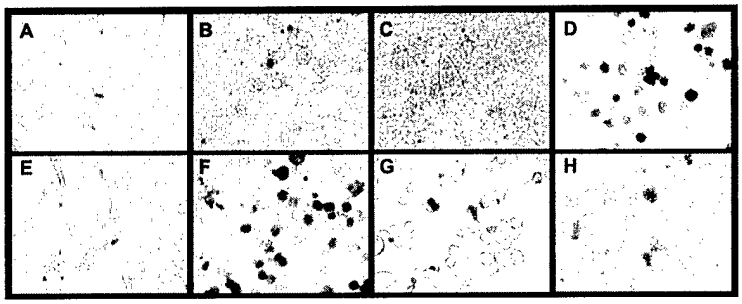


**Figure 2. TUNEL Assay of STS-induced Apoptosis.** The TUNEL stained cells were viewed and counted with a Lica microscope (model DM-IRB) and the pictures were acquired using an attached SPOT II digital camera. x400. The dark color co-localizing with nuclei represents TUNEL positive stain (converted to gray scale from the original brown color). The TUNEL positive cells in each sample were counted in 10 random fields and were presented as a percentage of the total number of cells counted (the number in parentheses). (A), untreated pCIneo (2.3 $\pm$ 1.7%); (B), STS-treated pCIneo cells (10 $\pm$ 2.4%); (C), untreated 70N cells (2.0 $\pm$ 1.2%; D, STS-treated 70N cells (44 $\pm$ 3.6%); (E), untreated Tn15 cells (2.7 $\pm$ 2.0%); (F), STS-treated Tn15 cells (54 $\pm$ 5.5%); (G), STS-treated maspin/PAI-1 transfectant clone #12 (19 $\pm$ 4.5%); (H), STS-treated PAI-1/maspin transfectant clone #5 (13 $\pm$ 2.0%). The untreated maspin/PAI-1 and PAI-1/maspin transfectants appeared similar to untreated Tn15 (data not shown).

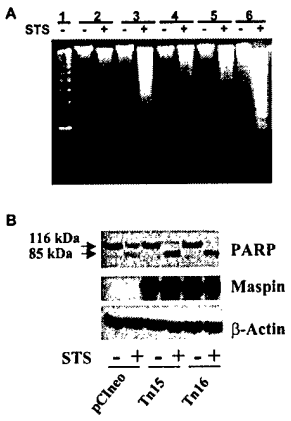


**Figure 3. DNA Fragmentation and PARP Inactivation.** (**A**) Agarose gel electrophoresis of DNA ladder. Lane 1 shows the DNA molecular weight marker. Samples 2-6 represent DNA isolated from untreated and STS-treated pCIneo, Tn15, Maspin/PAI-1 clone # 12, PAI-1/maspin transfectant clone #5, and normal mammary epithelial cells 70N, respectively. A total of 10 μg of DNA was loaded into each lane. (**B**) Western blotting of PARP and maspin. Cells were incubated in serum-free medium in the presence or absence of STS for 24 hours, and then lysed. A total of 100 μg of lysate protein from each cell line was resolved by SDS-PAGE and transferred to PVDF membrane, which was then probed with specific antibodies against PARP. The same blot was stripped and re-probed with the specific antibody against maspin. To assess the loading normality, the same blot was subsequently re-probed with the antibody against β-actin.

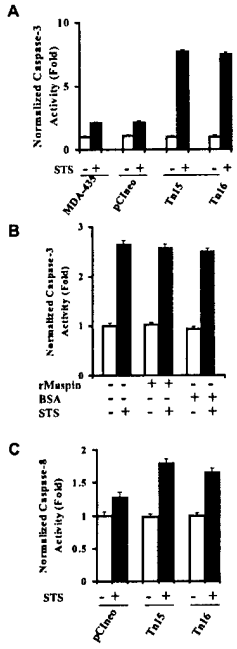


**Figure 4. The Activation of Caspases Following STS-induced Apoptosis.** (**A**) The effect of endogenous maspin on STS-induced caspase-3 activation. The production of fluorescent product in each cell lysate was normalized by, and expressed as fold increase of, that obtained with the lysate of untreated MDA-MB-435 cells. (**B**) The effect of purified rMaspin on caspase-3 activity. MDA-MB-435 cells were either untreated or treated with STS for 24 hours. The caspase-3 activity of the resulting cell lysates was measured in the presence or absence of 200 nM rMaspin in the assay mixtures. The caspase-3 activity (production of fluorescence) in each reaction is expressed as a fold increase compared to that obtained with untreated MDA-435 cells in the absence of rMaspin. Parallel reactions containing BSA at the final concentration of 200 nM was used as negative controls. (**C**) Shows the effect of endogenous maspin on STS-induced caspase-8 activation. The caspase activity (production of fluorescence) in each assay was expressed as fold increase of the corresponding caspase activity in the lysate of pCIneo cells. Values in (**A**)-(**D**) represent the average of three parallel experiments and the error bars represent the standard errors.

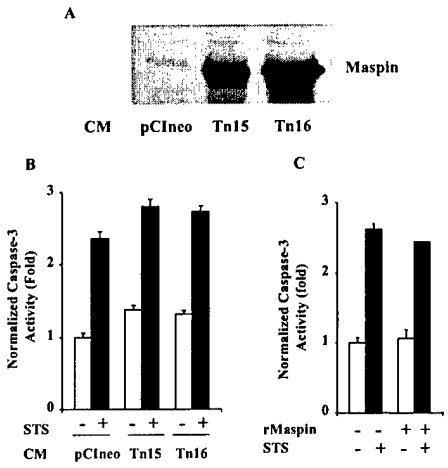


**Figure 5. The Effect of Extracellular Maspin on STS-induced Apoptosis.** (**A**) Detection of secreted maspin. Fifty micrograms of protein from the concentrated SF-CM of pCIneo or maspin transfectants (Tn15 and Tn16) were subjected to western blotting using a maspin-specific antibody. (**B**) The effect of extracellular maspin on STS-induced caspase-3 activation. pCIneo cells cultured in the media that was pre-conditioned by pCIneo, Tn15 and Tn16 cells, respectively, were either left untreated or treated with STS for 24 hr. The resulting cell lysates were analyzed by caspase-3 activity assay. The caspase-3 activity (fluorescence production) in each sample was expressed as a fold increase compared to that obtained with untreated pCIneo cells cultured in their own conditioned media. (**C**). The effect of purified rMaspin on STS-induced caspase-3 activation. MDA-MB-435 cells were induced by STS in the presence or absence of 200 nM rMaspin for 24 hr. The resulting cell lysates were analyzed by caspase-3 activity assay. The caspase-3 activity (fluorescence production) in each sample was expressed as a fold increase compared to that obtained with untreated cells in the absence of rMaspin. In both (**B**) and (**C**), the data represent the average of three parallel experiments and the error bars represent the standard errors.

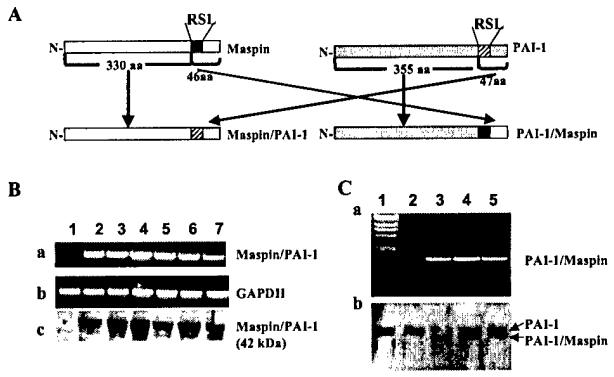


**Figure 6. The Construction and Endogenous Expression of Maspin/PAI-1 and PAI-1/Maspin Chimeras.** (**A**) The schematic diagram showing the construction of the maspin/PAI-1 and PAI-1/maspin chimeras by domain-specific fusion between maspin and PAI-1. (**B**) The expression of the maspin/PAI-1 chimera in MDA-MB-435 derived stable transfectant clones was detected by RT-PCR (a). Parallel RT-PCR for the housekeeping gene GAPDH was performed to assess the loading normality (b). The maspin/PAI-1 chimera protein in the cell lysates was detected by western blotting using a monoclonal antibody against maspin (c) (50 μg of protein/lane). In (a)-(c), lane 1 represents samples from a pCIneo clone, while lane 2 to 7 represent samples from maspin/PAI-1 transfectant clones #2, #5, #7, #8, #10, and #12, respectively. (**C**) The expression of PAI-1/maspin chimera in MDA-MB-435 derived stable transfectant clones was detected by RT-PCR (a). The PAI-1/Maspin chimera protein in the cell lysates was also detected by western blotting using monoclonal antibody EGG against PAI-1 (b). In (a) and (b), lane 2 represents samples from a pCIneo clone, while lane 3 to 5 represent samples from PAI-1/maspin transfectant clones #5, #6 and #12, respectively. Lane 1 in (a) shows the molecular markers of DNA (from top to bottom: 23 kb, 9.5 kb, 6.5 kb, 4.3 kb, 2.3 kb and 2.0 kb). Lane 1 in (b) was loaded with 0.5 μg of recombinant PAI-1. In (**B**) and (**C**), equal loading of western blots was verified by re-probing the membranes with β-actin antibody (data not shown).

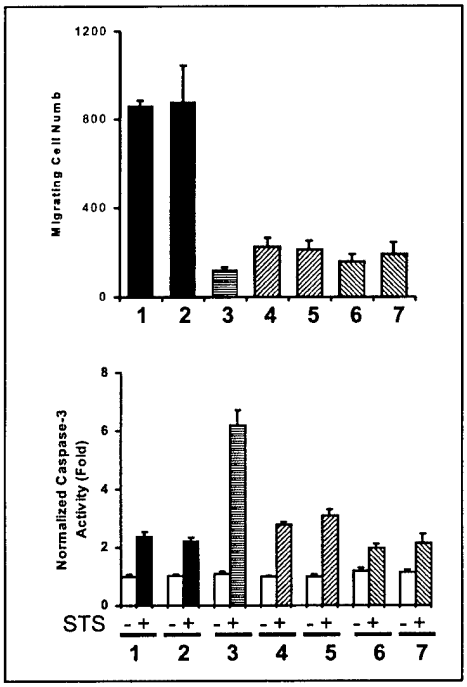


**Figure 7. The Effects of Maspin/PAI-1 and PAI-1/maspin on Cell Motility and STS-induced Apoptosis.** (**A**) *In vitro* cell motility assay. Cell motility is presented as total number of cells that migrated across the matrigel-coated polycarbonate filters. (**B**) Caspase-3 activities (productions of fluorescence) in cell lysates were expressed as fold increase compared to that obtained with the untreated parental MDA-MB-435 cells. Columns 1-7 in both (**A**) and (**B**) represent the average results of three parallel experiments with parental MDA-MB-435, pCIneo, Tn15, maspin/PAI-1 transfectant clone #5, maspin/PAI-1 transfectant clone #12, PAI-1/maspin transfectant clone #5, and PAI-1/maspin transfectant clone #6, respectively. The error bars represent the standard errors.

## PART II

**Bax Mediates the apoptosis-sensitizing effect of maspin**

Jiayou Liu, Shuping Yin, Craig Spencer and Shijie Sheng

Submitted to J. Biol. Chem. for publication (2003).


### ABSTRACT

Maspin, a serine protease inhibitor (serpin), can suppress tumor growth and metastasis *in vivo* and tumor cell motility and invasion *in vitro* (Zou et al., *Science,* 1994, 263: 526-9; Sheng et al., *PNAS USA*, 1996, 93:11669-74). This may occur through maspin-mediated inhibition of cell surface-bound uPA (McGowen et al., *Cancer Res.,* 2000, 60: 4771-8; Biliran et al., *Cancer Res.,* 2001, 61: 8676-82). Meanwhile, in a recent report, we provided the first evidence that maspin may also suppress tumor progression by enhancing cellular sensitivity to apoptotic stimuli (Jiang et al., *Oncogene,* 2002, 21: 4089-98). To our knowledge, maspin is the only proapoptotic serpin amongst all serpins so far implicated in apoptosis regulation. The goal of this current study is to identify the specific target molecule(s), the modification of which by maspin renders tumor cells sensitive toward chemotherapeutic agents. Our cellular, molecular and biochemical studies demonstrates an essential role of Bax in the proapoptotic effect of maspin. First, Bax was up-regulated in maspin transfected prostate and breast tumor cells while the levels of other Bcl-2 family members including Bcl-2, Bcl-xl, and Bak remained unchanged. Second, upon apoptosis induction, a greater amount of Bax was translocated from cytosol to mitochondria in maspin transfected cells. Consistent with a dominant role of the mitochondria pathway in the maspin effect, the release of Cytochrome c and Smac/DIABLO from mitochondria was more responsive to apoptosis stimuli in maspin transfected cells than in the mock transfected cells. Third, the apoptosis induction of maspin transfected cells was associated with increased activation of both caspase-8 and caspase-9. However, a caspase-9 specific inhibitor dose- and time-dependently blocked the sensitization effect of maspin, demonstrating a rate-limiting role of caspase-9. In line with the central role of Bax-mediated mitochondrial apoptotic pathway, maspin sensitized the apoptotic response of breast and prostate carcinoma cells to various types of stimuli, ranging from death ligands to endoplasmic reticulum (ER) stress. The link of maspin with Bax up-regulation helps explain the loss of maspin-expressing tumor cells in invasive breast and prostate carcinomas. Furthermore, our data suggest a novel mechanism, thus clinical application, of tumor suppressive maspin.


### INTRODUCTION

Maspin is a tumor suppressive serine protease inhibitor (serpin). Accumulated functional evidence demonstrates that maspin blocks tumor metastasis *in vivo* and tumor cell motility and invasion *in vitro* (1-3). In line with its sequence homology with many serpins (2), maspin can inhibit cell surface-bound urokinase plasminogen activator (uPA) in prostate tumor cells (4, 5). The maspin effect on pericellular uPA activity may underlie its stimulatory effect at the step of cell adhesion (6, 7), and its inhibitory effect on cell invasion and motility (4, 5). It is well documented that uPA, together with its cell surface receptor uPAR, are up-regulated in invasive and metastatic carcinomas. Interestingly, plasminogen activator inhibitory type 1 (PAI-1), a known uPA inhibitor, is also up-regulated along with uPA in invasive cancers (8). In contrast, we have shown that maspin expression is lost at the critical transition from non-invasive to invasive breast and prostate carcinomas (2, 9, 10). This result has been recently confirmed by a microarray analysis by Chen et al (10). Interestingly, maspin expression is also inversely correlated with transmembrane type serine protease hepsin, raising the possibility that maspin may cross-inhibit transmembrane serine proteases, as well.

It is important to point out, however, in several *in vivo* studies that maspin-expressing tumor cells were inhibited in gross growth (2, 3, 11). However, the effect of maspin on tumor growth was not reproduced by *in vitro* cell culture experiments, suggesting that an inhibitory effect of maspin on tumor cell survival or growth may be further dependent on additional stimuli from the tumor microenvironment. In a recent report, we provided the first evidence that endogenous maspin expression sensitizes breast carcinoma cells to staurosporine (STS)-induced apoptosis *in vitro* (12). To our knowledge, this is also the first evidence that a mammalian serpin can act as an apoptosis antagonist. The apoptosis-sensitizing effect of maspin appears to be an intracellular, rather than extracellular. Furthermore, as compared to the extracellular effect of maspin that depends on its reactive site loop (RSL) sequence, the intracellular maspin effect on apoptosis depends both on its RSL and its N-terminal domain (12). These results suggest that the concerted activities of intracellular and extracellular maspin may help eliminate invasive carcinoma cells, and help explain the evidence that (i) maspin exerts dual inhibitory effects on tumor growth and metastasis *in vivo* (2, 3, 11); and (ii) the loss of maspin in the progression of breast and prostate cancers coincides with the transition from non-invasive to invasive lesions (2, 9).

To further explore the potential application of maspin in apoptosis-based cancer intervention, it is of fundamental importance to identify the molecular mechanism underlying its proapoptotic effect. Apoptosis, in general, consists of three steps: induction, commitment and execution. The mechanism of induction can be intrinsic or extrinsic, depending on each specific apoptotic inducer. The commitment of apoptosis is largely a mitochondrial event controlled by proteins in the Bcl-2 family (13-15). The antiapoptotic members of the Bcl-2 family (e.g., Bcl-2 and Bcl-xl) protect against mitochondrial membrane disruption, whereas the proapoptotic members (e.g., Bax and Bak), that undergo cytosol to mitochondria translocation in response to death signal, cause mitochondrial release of apoptogenic factors such as Cytochrome c (16, 17) and Smac/DIABLO (18, 19). Thus, the relative concentration of anti- *vs.* proapoptotic members of the Bcl-2 family may act as a rheostat for the death program. The execution of apoptosis features a series of common events including activation of effector caspases. In particular, the Cytochrome c released into cytosol leads to Apaf-1-mediated apoptosome assembly and a rapid activation of caspase-9 (16, 17), whereas Smac/DIABLO interacts with inhibitors of apoptotic proteases (IAPs, e.g., XIAP), and thus block their inhibitory effects on activated caspase-9 and caspase-3 (18, 19). Caspase-3 cleaves many cellular proteins, ultimately leading to nuclear DNA fragmentation and cytoskeleton collapse (13-15).

In the current study, we described cellular, molecular and biochemical evidence that the apoptosis-sensitizing effect of maspin, which was independent of apoptosis inducers, resulted predominantly from increased Bax expression and activity. These results suggest that maspin may be useful to restore tumor sensitivity toward a broad range of apoptosis-based chemotherapies.

## RESULTS

### Maspin Sensitizes Apoptotic Response of Prostate Carcinoma Cells to Distinct Stimuli.

Maspin has been shown to sensitize breast carcinoma cells MDA-MB-435 to staurosporine (STS)-induced apoptosis (12). To further explore the potential of maspin as an agonistic modifier of cancer chemotherapeutic agents, it is critical to investigate (i) whether maspin sensitize apoptotic response in other types of cancer cells, and (ii) whether the maspin effect depends on specific apoptosis inducers. In the current study, we extended our investigation to prostate carcinoma cells DU145-derived stable maspin transfected clones (4). We have previously reported that expression of maspin in these transfectant cells resulted in reduced cell motility and invasion without altering cell growth kinetics in culture (4), a finding similar to that with MDA-MB-435-derived maspin transfectanted cells (12). When

treated with STS, the maspin-expressing clone M7 exhibited concentration- and time-dependent phenotypic changes typical of apoptosis, including cell shrinkage and detachment (data not shown). Six hours after the treatment, M7 had undergone significant nuclear DNA condensation and fragmentation as revealed by a Hoechst fluorescent staining method (Figure 1A). In contrast, the mock transfected control Neo cells were markedly more resistant to STS-induced apoptosis. In fact, after the same treatment, some Neo cells remained mitotic. As summarized in Figure 1B, STS treatment produced approximately 3 times more apoptotic cells in M7 than in Neo cells. Notably, the numbers of apoptotic M7 and Neo cells were similarly insignificant when untreated.

STS is a synthetic chemical known to induce apoptosis via an intrinsic pathway, presumably by changing the mitochondria membrane permeability (20). To test whether maspin regulates tumor cell response to pathophysiological apoptosis inducers such as extrinsic TRAIL or TNF-α, M7 and Neo cells were treated with TRAIL, an exclusive apoptotic cytokine (21). Ninety minutes into the treatment, more than 70% of M7 cells showed nuclear DNA fragmentations to various extents. In contrast, only 13% of TRAIL-treated Neo cells underwent significant nuclear DNA fragmentation (Fig. 1B). Similar differential responses were observed when M7 and Neo cells were treated with TNF-α for 3 hours in the presence of cycloheximide (CHX). TNF-α/CHX induced apoptosis was further verified at the molecular level by the specific cleavage of 116 kDa PARP to its 85 kDa product (Figure 1C). Although clonal variation was observed, all these maspin transfected clones (M3, M7, and M10) were significantly more sensitive than Neo cells. In M7, in particular, the 85 kDa fragment became the predominant PARP species detected. The extents of PARP cleavage semi-quantitatively correlated with the morphological changes of the nuclei in the corresponding cell lines (data not shown).

Apoptosis may also result from endoplasmic reticulum (ER) stress (22). Brefeldin A, for example, inhibits ER-Golgi transport and induces ER-stress and apoptosis. To test the effect of maspin on ER-stress induced apoptosis, M7 and Neo cells were treated with brefeldin A. As compared to Neo cells, M7 cells underwent more rapid cell shrinkage and detachment (data not shown). Furthermore, among the remaining adherent cells, approximately one third of M7 cells showed nuclear DNA fragmentation, while only 14% of Neo cells were positive for nuclear DNA fragmentation (Fig. 1B). In parallel, thapsigargin, another cytotoxic ER-targeting drug, induced similar differential responses in M7 and Neo cells (data not shown). Taken together, these results demonstrate that the maspin effect on apoptosis is independent of the types of death stimuli, and suggest that maspin may regulate a step downstream of the converging point for extrinsic and intrinsic pathways.

**Maspin Expression Correlates with Increased Activation of Caspase-9, Caspase-8 and Caspase-3.** To identify the specific apoptotic step(s) regulated by maspin, we first examined the effect of maspin on caspase-3 by a fluorogenic DEVDase assay. Upon TRAIL treatment, M7 cells exhibited a rapid increase in caspase-3 activation in the first 30 min (Fig. 2A). The caspase-3 activation in Neo cells, however, started after a 30-min attenuation. Moreover, the maximum caspase-3 activity in Neo cells was about 3/5 of that in M7 cells. Then, caspase-3 activity started to decrease in both cell lines, reflecting the loss of apoptotic cells to complete cell death. In parallel, TNF-α/CHX-treated M7 cells exhibited a rapid increase in caspase-3 activity starting from the second hour of treatment (Fig. 2B). The caspase-3 activity in Neo cells, on the other hand, started to increase after a 2-hour attenuation period and reached the maximum level 5 hours after the induction. The maximum caspase-3 activity in Neo cells was approximately 2/3 of that in M7. It was noted that although maspin indiscriminatingly sensitized cellular apoptotic response to TRAIL and TNF-α, the effect of maspin did not diminish the difference between these two death ligands in their cytotoxicities. These results further demonstrate the maspin independence of apoptotic stimuli.

Previously, we showed that maspin does not directly inhibit or activate caspase-3 (12). In this study, M7 cells and Neo cells expressed comparable amount of caspase-3 protein as judged by western blotting analyses (data not shown). Further, as shown in Figure 3A, the endogenous caspase-inhibitor XIAP was altered by maspin transfection. Thus, the differential kinetics of caspase-3 activation in M7 cells and Neo cells might result from differential activities of caspase-3 activating enzyme(s) in these two cell populations. Caspase-9 is a known caspase-3 activating enzyme in both intrinsic and extrinsic apoptotic pathways. Real-time PCR detection of caspase-9 showed that the expression of caspase-9 at the RNA level was not different in all clonal cell lines tested (data not shown). Western blotting, however, showed significantly less procaspase-9 in untreated M3 and M7 cells than in untreated Neo cells (Figure 3B). The reduction of procaspase-9 might be due to autoproteolytic activation of the enzyme (23). Consistent with this notion, upon TRAIL treatment (50 ng/ml/50 min), the remaining procaspase-9 was further reduced in M3 and M7 while it remained largely unchanged in Neo cells. The 50 min treatment was chosen because the difference of caspase-3 activity between M7 and Neo cells was maximal at this time point (Figure 2A).

Caspase-8 is another major caspase-3 activating enzyme. Both TRAIL and TNF-α are known to bind to their cell surface receptors, leading to caspase-8 activation. Activated caspase-8, in turn, may directly activate caspase-3, and indirectly activates caspase-9 via a mitochondrial-dependent mechanism (24). The expression of TRAIL receptors (DR4 and DR5) and TNF-α receptor (TNR2) was indifferent between maspin transfected cells and the mock control cells, as judged by western blots (data not shown). Western blotting was performed using an antibody that recognizes both pro- and activated caspase-8. As shown in Figure 3C, untreated M3, M7 and Neo cells expressed procaspase-8 protein at a comparable level. The same 50 min TRAIL treatment led to a greater reduction of procaspase-8 in M3 and M7 cells than in Neo cells. Conversely, a greater amount of activated caspase-8 (i.e., p43/36 and p23) was found in M3 and M7 cells than in Neo cells. These data indicate that the death receptor-mediated proteolytic activation of caspase-8 was enhanced by maspin expression.

**Mitochondrial Pathway Is Essential for the Proapoptotic Effect of Maspin.**

Using a caspase-9 specific fluorogenic substrate, we found that the caspase-9 activity increased more than 3 fold in TRAIL-treated M7 cells, but remained at the basal level in TRAIL-treated Neo cells (Figure 4A). In similar biochemical assays using a caspase-8 specific fluorogenic substrate, caspase-8 activity was barely detectable in all clonal cell lines tested (data not shown). The discrepancy between this result and the western blotting of caspase-8 (Figure 3C) may be due to different sensitivities of each assay. Alternatively, it is possible that caspase-9 was enzymatically more important for the proapoptotic effect of maspin. To further assess the relative significance of caspase-8 and caspase-9 in caspase-3 activation, caspase-3 activity was determined after apoptosis was induced in the presence of z-LEHD-fmk, an inhibitor of caspase-9 (25), or z-VAD-fmk, a general inhibitor of most caspases (25, 26). As shown in Figure 4B, TRAIL alone induced a dramatic increase of caspase-3 activity in M7 cells, while causing only a marginal increase of caspase-3 activity in Neo cells. The differential response of M7 and Neo cells was completely abolished not only by z-VAD-fmk, but also dose-dependently by z-LEHD-fmk. Western blotting of PARP further confirmed that z-LEHD-fmk eliminated TRAIL-induced cell death of M7 cells (Figure 4C) in a time-dependent fashion (Figure 4D). In parallel, when treated with TNF-α/CHX, M7 cells exhibited an increase of caspase-3 activity, twice as much as that found in Neo cells. Again, this differential response was completely abolished by z-LEHD-fmk at a final concentration of 50 μM. Taken together, these results suggest that the apoptosis-sensitizing effect of maspin may be mediated primarily by enhanced caspase-9 activation.

The release of mitochondrial factors such as Cytochrome c and Smac/DIABLO is considered a prerequisite for caspase-9 activation in apoptosis (16-19). Cytosolic presence of Cytochrome c leads to

Apaf-1-mediated apoptosome assembly and rapid activation of caspase-9 (16, 17), whereas Smac/DIABLO interacts with XIAP, and blocks its inhibitory effects on activated caspase-9 and caspase-3 (18, 19). We found that, when untreated, both M7 and Neo cells had little or no detectable Cytochrome c and Smac/DIABLO in the cytosol, as judged by western blots. However, upon TRAIL induction, cytosolic Cytochrome c and Smac/DIABLO quickly increased in M7 cells, whereas only a marginal increase of these molecules was observed in the cytosol of Neo cells (Figure 5A). Similar differential releases of Cytochrome c and Smac/DIABLO were observed upon induction by TNF-α/CHX or STS (data not shown). To examine whether Cytochrome c release was biologically functional in initiating apoptosome assembly, immunoprecipitation (IP) was performed with cytosolic preparations from TRAIL-treated cells using Cytochrome c antibody. As shown in Figure 5B, western blotting detected a significantly greater amount of Apaf-1 in Cytochrome c co-precipitates from M7 cells than from Neo cells. This data supports the notion that caspase-9 activation is essential in the maspin effect on apoptosis and suggest that maspin expression in tumor cells may alter the regulation of mitochondria membrane potential by the Bcl-2 family member proteins (13, 15, 27).

**Up-regulation of Bax in Maspin Transfected Cells Tips the Balance of Resistance and Sensitivity.**

Western blotting did not detect Bcl-2 in maspin transfected and mock transfected DU145 cells (data not shown). In addition, as shown in Figure 6A, Bcl-xl, an antiapoptotic Bcl-2 homologue, and Bak, a proapoptotic Bcl-2 homologue, were each expressed at comparable levels in M7 and Neo cells. Interestingly, a significantly higher amount of proapoptotic Bax protein was found in maspin transfected cells (M3, M 7, and M10), despite the noticeable clonal variations, as compared to that in Neo cells (Figure 6B). Neither TRAIL nor STS further affected the differential expression pattern of Bax between M7 cells and Neo cells (Fig. 6C). Additionally, MDA-MB-435-derived maspin transfectanted cells, that are more sensitive to STS-induced apoptosis (12), were found to express Bax at a significantly higher level than the corresponding mock control cells, while Bcl-2 and Bcl-xl expression remained the same in all those clonal cell lines tested (data not shown).

To further investigate the differential regulation of Bax expression in maspin transfected *vs.* mock control tumor cells, semi-quantitative RT-PCR was performed with total RNAs extracted from untreated cells. As shown in Figure 7A, the RNA from M7 and Tn 16 (maspin transfected MDA-MB-435 cells) gave rise to a more rapid amplification of Bax cDNA than the corresponding mock control RNA (Neo and Nn12, respectively), while GAPDH, a housekeeping gene commonly used as RNA loading control, was amplified equally in the same set of RNA samples. To confirm the difference in Bax expression, real- time PCR was performed multiple times using two different real-time thermal cyclers and independently prepared RNA samples. Reproducibly, the Bax amplification was significantly more rapid with the RNA of M7 cells than that of Neo cells (Fig. 7B). These data suggests that the up-regulation of Bax in maspin transfected cells may occur at the transcriptional level.

To investigate whether the higher amount of Bax protein present in maspin transfected cells was functionally relevant, we examined Bax localization. M7 and Neo cells were treated with TRAIL. The resulting cell lysates were subjected to fractional centrifugation to separate membrane bound and cytosolic fractions. As shown in Figure 8A, cytosolic Bax protein that was detected in untreated M7 cells largely disappeared after TRAIL treatment. Concomitantly, the Bax level significantly increased in the membrane fraction of TRAIL treated M7 cells as compared to that of untreated M7 cells. In Neo cells, Bax protein, albeit at a much lower level, also appeared to undergo translocation from cytosol to mitochondria. Immunofluorescent staining showed that, upon TRAIL (data not shown) or STS treatment (Figure 8B), most of the cytosolic Bax in M7 cells was translocated to perinuclear space with a punctuate staining pattern, typical for mitochondria localization. In Neo cells, Bax protein translocation was hardly detected by this method.

## DISCUSSION

To our knowledge, maspin is the only serpin that sensitizes apoptosis, while all other serpins so far implicated in apoptosis regulation appear to be antiapoptotic (14, 28, 29). Thus, the existing literature offers little insight into the possible molecular mode of maspin action. The goal of this current study was to identify the specific target molecule(s), the modification of which by maspin sensitizes prostate and breast tumor cells toward potential cancer chemotherapeutic agents. By using multiple maspin transfected cell lines *in vitro*, we obtained cellular, molecular and biochemical evidence that supports a key role of Bax in maspin-mediated apoptosis sensitization. Although we may not have exhausted our search due to the ever-growing number of apoptosis regulators, our data seems sufficient to support our new hypothesis that the specific up-regulation of Bax, without changing Bcl-2, Bcl-xl and Bak expression in maspin transfected cells, may tip the balance of pro- *vs.* antiapoptotic regulators, and potentiate mitochondrial membrane for apoptosis. In particular, the following considerations further support this hypothesis.

Bax overexpression predicts a predominant role of mitochondria in the maspin effect on apoptosis (30). Indeed, we found that the level of Bax expression and translocation correlated positively with mitochondrial Cytochrome c and Smac/DIABLO release, activation of caspase cascade from apical caspases to effector caspases, and nuclear phenotypes (PARP cleavage and DNA fragmentation). Bax overexpression may further predict an elevated cellular apoptotic response to a broad spectrum of apoptosis stimuli. We showed that maspin-expressing clones were sensitized to a broad range of apoptosis inducers, including TRAIL, TNF-α, STS, brefeldin A, thapsigargin. Although the early signaling pathways elicited by these inducers differ, they may all converge at the step of mitochondria membrane potentiation (13, 27). For example, STS is known to cause Bax translocation to mitochondria and disruption of mitochondria membrane pores in many different cells, leading to the release of mitochondrial factors (31, 32). Brefeldin A and thapsigargin, on the other hand, are commonly used to deplete the ER $Ca^{2+}$ pool, causing extensive ER stress. The $Ca^{2+}$ released from ER is rapidly accumulated in mitochondria (33, 34), leading to a decrease in mitochondrial transmembrane potential, and the release of mitochondrial factors (33-37). Consistently, antiapoptotic Bcl-2 has been shown to inhibit death stimuli-induced increase of $Ca^{2+}$ concentration in mitochondria (38).

The mode of death ligand action (e.g., TRAIL, TNF-α) seems to be complex. A body of evidence argues that they inflict apoptosis by first activating caspase-8 through the death inducing signaling complex (DISC) (39, 40). The amplification of down-stream death signal, however, may involve Bcl-2 family protein-mediate mitochondrial pathways (41). Thus, it was not surprising that TRAIL and TNF-α induced activation of both caspase-8 and caspase-9 as observed in this study. To date, there is no evidence for a direct regulatory role of maspin in death receptor-mediated DISC activity. On the other hand, emerging evidence suggests that activation of caspase-8 in TRAIL (or TNF-α)-induced epithelial apoptosis may also be mediated by a mitochondria-dependent mechanism (42). Considering (i) the up-regulated Bax expression in maspin transfected cells and (ii) the increase of caspase-8 activation in MDA-MB-435 derived maspin transfected cells following a treatment with STS, a non-death ligand type apoptotic inducer (12), we speculate that the increased caspase-8 activation in these cells was a result of the increased mitochondrial apoptotic activities. It is important to note that despite the increased caspase-8 activation in maspin transfected cells, a caspase-9 specific inhibitor completely abolished the enhanced caspase-3 activation and PARP cleavage in these cells (Figure 4). Although we cannot exclude the possibility that caspase-8 may cleave other substrates such as Bid (43, 44) and cytoskeletal protein plectin (45), and further facilitate the apoptosis to completion, our data so far support that caspase-9, but not caspase-8, was the predominant apoptosis executing enzyme.

High levels of Bax expression may be sufficient to confer apoptosis (46). Interestingly, the up-regulated Bax expression did not lead to spontaneous apoptosis of maspin transfected cells. Cell lysates extracted from untreated maspin transfected cells did not possess a higher level of caspase-9 activity (Figure 4), even though more procaspase-9 protein appeared to be cleaved as compared to that in the untreated mock control cell (Figure 3). Furthermore, the proteolytic cleavage of procaspase-9 in maspin-expressing cells prior to apoptosis induction was not accompanied by Cytochrome c and Smac/DIABLO release (Figure 5). It is possible that the observed caspase-9 cleavage was not a part of, or sufficient for, caspase-9 activation. Alternatively, this proteolytic cleavage might have yielded active caspase-9, which was quickly neutralized by its cognate inhibitor such as XIAP. To this end, evidence exists that the potency of the proapoptotic effect of Bax may be fine-tuned by the balanced release of Cytochrome c and Smac/DIABLO from mitochondria. Cytochrome c and Smac/DIABLO release are respective prerequisites for caspase-9 activation and XIAP inactivation (16-19, 46). A rapid execution of apoptosis occurs when activation of caspase-9 and inactivation XIAP are provoked simultaneously. In the absence of apoptotic stimuli, an increased cytosolic presence of Bax in close vicinity of mitochondria may be sufficient to cause incidental mitochondrial leakage, which may allow selectively small molecules such as Cytochrome c, but not large proteins like Smac/DIABLO, to escape (27). The imbalanced release of Cytochrome c and Smac/DIALBO would lead to a higher level of active caspase-9 without causing apoptosis due to the overwhelming inhibitory effect of XIAP.

The overexpression of Bax in maspin transfected cells appeared to be regulated at a step prior to protein translation. Current evidence suggests the following two mechanisms by which maspin may affect Bax expression at the transcriptional level. A recent study by Odero-Marah showed that maspin underwent epidermal growth factor receptor-mediated tyrosine-phosphorylation *in vitro* (47). In addition, a fraction of maspin protein seems to localize in cell nuclei (48). It remains to be seen whether intracellular maspin may directly regulate the signal transduction, leading to increased Bax expression. Alternatively, it has been shown that mitogen activated protein kinase (MAPK) plays a central role in cell survival, in part, by down-regulating the expression of proapoptotic genes such as Bax (49, 50). Among the increasing number of proteins that regulate MAPK activation, the uPA/uPAR complex has been shown to activate p38, through its interaction with integrins, and subsequently leads to activation of MAPK (51, 52). Since endogenous maspin expression in tumor cells not only inhibits pericellular uPA activity, but also dramatically reduces cell surface-associated uPA and uPAR proteins via rapid Lipoprotein Receptor Related Protein (LRP)-mediated internalization (4), it is possible that constitutive expression of maspin positively regulates Bax transcription by eliminating the signal transduction from uPA/uPAR to MAPK.

In summary, our detailed biochemical and molecular analyses lead to the identification of Bax as a key effector of maspin in the regulation of cellular apoptotic sensitivities. This finding helps explain the general sensitizing effect of maspin on cellular response to multiple apoptotic inducers that act by distinct mechanisms. Currently, a barrier for designing apoptosis-based therapies is that many types of tumors manifest a substantial drug resistance due to an unfavorable Bcl-2/Bax ratio (53). Results of this study suggest that re-expression of maspin in tumor cells may reverse or reduce drug resistance. It is important to bear in mind that maspin is expressed in and, therefore, tolerated by benign epithelial cells in breast and prostate glands that still have supportive and relatively inactive stroma. "Maspin expression" is shown to be lost in invasive breast and prostate carcinomas (2, 9). In view of (i) our evidence that maspin did not provoke, but rather sensitized tumor cell apoptotic responses and (ii) clinical observation that invasive cancers are often associated with highly immunoreactive stroma marked with increased secretion of cytokines such as TNF-$\alpha$ (54-57), it is likely that maspin-expressing tumor cells, but not the maspin expression in tumor cells, are selected out in tumor progression.

Consistent with this notiton, oxidative stress-induced apoptosis in breast cancer cells, following manganese-containing superoxide dismutase overexpression, was associated with an elevated level of maspin expression (58). Taken together, our data suggest a novel mechanism for the tumor suppressive activity of maspin. Moreover, the reactive stroma in invasive prostate and breast carcinomas may offer a unique advantage in maspin-based therapies for achieving a greater tumor specific toxicity.

## METHODS

**Cell Culture and Apoptosis Induction.** Clonal cell lines M3, M7 and M10 were derived from stable transfection of human prostatic carcinoma cells DU145 with maspin cDNA (4). Clonal cell line Neo was derived from stable transfection of DU145 cells with the mock vector. Tn16 and Nn12 were maspin transfected and mock transfected clonal cell lines, respectively, derived from breast carcinoma cells MDA-MB-435 (1). These cells were maintained as previously described (1, 4).

Routinely cells were grown to 80-90% confluence prior to treatments. Inducers of apoptosis used include 50 ng/ml TRAIL, 50 ng/ml TNF-α in combination with 2 μg/ml of cycloheximide (CHX), 1 μM staurosporine (STS), and 30 μg/ml brefeldin A. When cells were additionally treated with caspase inhibitor z-VAD-fmk or z-LEHD-fmk (BD Biosciences, San Diego, CA), these inhibitors were added 1 or 2 h as indicated before apoptotic induction. TRAIL and TNF-α were purchased from R&D Systems (Minneapolis, MN). STS, brefeldin A and CHX were obtained from SIGMA (St Louis, MO).

**Detection of Apoptosis.** For evaluation of nuclear morphology, cells were fixed with methanol and stained with the DNA dye bisbenzimide (Hoechst 33258, SIGMA). Cells with fragmented nuclei were then counted under a Leica fluorescence microscope (Model DM IRM). Caspase activities were determined by fluorogenic assays as described previously (12).

**Western Blotting and Immunoprecipitation.** For western blotting analysis, cell lysates were, unless otherwise specified, prepared with a low salt buffer as described (4). Antibodies used include: PARP (BIOMOL, Plymouth Meeting, PA), DR4, DR5 and TNR2 (Oncogene, San Diego, CA), Apaf-1, and XIAP (Transduction Laboratories, San Diego, CA), caspase-8, Cytochrome c and Smac/DIABLO (PharMingen, San Diego, CA), caspase-9 (Calbiochem, San Diego, CA), Bcl-2 and Bcl-xl (Santa Cruz Biotech, Santa Cruz, CA), Bak (UPSTATE, Lake Placid, NY). Bax antibody in the western blotting with fractionated cell lysates (Figure 8) was a monoclonal antibody purchased from Santa Cruz Biotech. The Bax antibody used in all other experiments was a polyclonal antibody obtained from UPSTATE. Anti-β-actin (Sigma, St. Louis, MO) was used for loading controls. Immunoprecipitation (IP) was performed as described (59). Briefly, cytosolic fractions were incubated overnight with the Cytochrome c antibody. Immune complexes were precipitated with protein A/G-Sepharose beads and washed with lysis buffer before being resolved on SDS-PAGE.

**Subcellular Fractionation.** Cytosolic fractions and mitochondria-enriched fractions were prepared as described (60). Briefly, cells were collected in sucrose buffer (300 mM sucrose/10 mM Hepes, pH 7.4/50 mM KCl/5 mM EGTA/5 mM $MgCl_2$/1 mM DTT). The cells were then homogenized in five strokes with a Dounce homogenizer. The remaining intact cells and nuclei were removed by centrifugation at 1,000 × *g* for 10 min at 4 °C. The supernatants were spun at 14,000 × *g* for 15 min at 4 °C to separate mitochondria-enriched pellets and cytosolic supernatants. The mitochondrial pellets were rinsed twice with the sucrose buffer and solublized in the low salt buffer supplemented with 1% Triton X-100 and 0.5% SDS. Western blots probed with antibody for the mitochondrial resident protein mtHSP70 (Bioreagents, Golden, CO) and anti-β-actin antibody were performed to normalize the loading of mitochondrial and cytosolic proteins, respectively.

**Immunofluorescence Microscopy.** Cells cultured on chamber slides were washed twice with phosphate-buffered saline (PBS), fixed in 3.8% formaldehyde for 10 min and permeabilized with 0.1%

Triton-X-100 for 5 min. After three more washes, cells were blocked with 2% bovine serum albumin (BSA) for 1 h before incubated with polyclonal antibody for Bax (UPSTATE) at 4 °C overnight. Cells were then washed five times, followed by incubation with 1/500 dilution of Oregon Green-conjugated goat anti-rabbit secondary antibody (Molecular Probes, Eugene, OR) for 1 h. Cells were mounted using Prolong Antifade solution (Molecular Probes). Confocal microscopy examination was performed using Zeiss LSM 310 model (The Imaging Core Facility of the Karmanos Cancer Institute, Detroit, MI).

**RT-PCR and Real-time PCR Analyses.** Total RNA was extracted as described (4). The quality of the RNA preparations was verified by agarose gel electrophoresis showing intact 18S and 28S rRNA, and by UV spectrophotometry showing an optimal A260/280 ratio (close to 2). One microgram of each total RNA sample was reverse transcribed in a 20 μl reaction as described (4). A total of 5 μl of 5-fold diluted cDNA products was used in semiquantitative PCR experiments using 200 nM gene-specific primers. The primers for Bax were 5'-ATCCAGGATCGAGCAGGGCG and 5'-GGTTCTGATCAGTTCCGGCA. The GAPDH primers were as described (4). The PCR conditions were 1 min at 90 °C, 35 cycles (for Bax), or 25 cycles (for GAPDH), of 15 s at 94 °C, 20 s at 60 °C and 1 min at 72 °C. The resulting products were visualized by agarose gel electrophoresis followed by ethedium bromide staining.

For real-time PCR, SYBR Green PCR Core Reagents (PE Biosystems, Warrington, UK) were used together with 3 μl of the aforementioned diluted cDNA and 200 nM of primers for Bax and GAPDH, respectively. The real-time PCR conditions were 2 min at 50 °C, 10 min at 95 °C, 35 cycles of 10 s at 95 °C and 1 min at 60 °C. Four independent runs were carried out in two different real-time PCR cyclers (Smart Cycler, Cepheid, Sunnyvale, CA; I-cycle, Biorad, Hercules, CA) to confirm the reproducibility. For analysis, a threshold of arbitrary fluorescence reading was set at 30 at which the increase in fluorescence exceeded the background noise and entered into the exponential phase. The fluorescence readings were taken when the slower reaction in the pairs reached the threshold cycle. The real-time PCR for GAPDH was used as a normalization control.

## ACKNOWLEDGEMENTS

We greatly appreciate the proofreading of the manuscript by Drs. Fayyaz Ahmed, Yonghong Meng, Mr. Jaron Lockett and Ms. Debbrah Leicht. This work was supported by NIH grant CA84176, DOD grant BC0996974 and the Ruth Sager Memorial Fund (all to S.S.).

## REFERENCES

1. Sheng S, Carey J., Seftor E, Dias L, Hendrix MJC, Sager R (1996) *Proc. Natl. Acad. Sci. USA,* **93,** 11669-11674.
2. Zou Z, Anisowicz A, Hendrix MJC, Thor A, Neveu M, Sheng S, Rafidi K, Seftor E, Sager R (1994) *Science,* **263,** 526-529.
3. Zhang M, Volpert O, Shi YH, Bouck N (2000) *Nat Med,* **6,** 196-199.
4. Biliran H Jr, Sheng S Pleiotrophic (2001) *Cancer Res,* **61,** 8676-8682.
5. McGowen R, Biliran H Jr, Sager R, Sheng S (2000) *Cancer Res,* **60,** 4771-4778.
6. Abraham S, Zhang W, Greenberg N, Zhang M (2003) *J Urol,* **169,** 1157-1161.
7. Seftor RE, Seftor EA, Sheng S, Pemberton PA, Sager R, Hendrix MJ (1998) *Cancer Res,* **58,** 5681-5685.
8. Sheng, S (2001) *Cancer Metastasis Rev,* **20,** 287-296.
9. Pierson CR, McGowen R, Grignon D, Sakr W, Dey J, Sheng S (2002) *Prostate,* **53,** 255-262.
10. Chen Z, Fa Z, McNeal JE, Nolley R, Caldwell MC, Mahadevappa M, Zhang Z, Warrington JA, Stamey TA (2003) *J Urol,* **169,** 1316-1319.

11. Sager R, Sheng S, Anisowicz A, Sotiropoulou G, Zou Z, Stenman G, Swisshelm K, Chen Z, Hendrix MJ, Pemberton P, et al (1994) *Cold Spring Harb Symp Quant Biol,* **59,** 537-546.
12. Jiang N, Meng Y, Zhang S, Mensah-Osman E, Sheng S (2002) *Oncogene,* **21,** 4089-4098.
13. Green DR, Reed JC (1998) *Science,* **281,** 1309-1312.
14. Zhou HM, Bolon I, Nichols A, Wohlwend A, Vassalli JD (2001) *Cancer Res,* **61,** 970-976.
15. Adams JM, Cory S (1998) *Science,* **281,** 1322-1325.
16. Liu X, Kim CN, Yang J, Jemmerson R, Wang X (1996) *Cell,* **86,** 147-157.
17. Li P, Nijhawan D, Budihardjo I, Srinivasula SM, Ahmad M, Alnemri ES, Wang X (1997) *Cell,* **91,** 479-489.
18. Du C, Fang M, Li Y, Li L, Wang X (2000) *Cell,* **102,** 33-42.
19. Verhagen AM, Ekert PG, Pakusch M, Silke J, Connolly LM, Reid GE, Moritz RL, Simpson RJ, Vaux DL (2000) *Cell,* **102,** 43-53.
20. Duan S, Hajek P, Lin C, Shin SK, Attardi G, Chomyn A (2003) *J Biol Chem,* **278,** 1346-1353.
21. Smyth MJ, Takeda K, Hayakawa Y, Peschon JJ, van den Brink MR, Yagita H (2003) *Immunity,* **18,** 1-6.
22. Nakagawa T, Zhu H, Morishima N, Li E, Xu J, Yankner BA, Yuan J (2000) *Nature,* **403,** 98-103.
23. Kuida, K (2000) *Int J Biochem Cell Biol,* **32,** 121-124.
24. Kruidering M, Evan GI (2000) *IUBMB Life,* **50,** 85-90.
25. Gregoli PA, Bondurant MC (1999) *J Cell Physiol.,* **178,** 133-143.
26. Schrantz N, Blanchard DA, Auffredou MT, Sharma S, Leca G, Vazquez A (1999) *Oncogene,* **18,** 3511-3519.
27. Wang, X (2001) *Genes Dev.,* **15,** 2922-2933.
28. Gabriel C, Ali C, Lesne S, Fernandez-Monreal M, Docagne F, Plawinski L, MacKenzie ET, Buisson A, Vivien D (2003) *FASEB J,* **17,** 277-279.
29. Dickinson JL, Norris BJ, Jensen PH, Antalis TM (1998) *Cell Death Differ,* **5,** 163-171.
30. Hardwick JM, Polster BM (2002) *Mol Cell,* **10,** 963-965.
31. Hsu YT, Wolter KG, Youle RJ (1997) *Proc. Natl. Acad. Sci. U. S. A.,* **94,** 3668-3672.
32. Wolter KG, Hsu YT, Smith CL, Nechushtan A, Xi XG, Youle RJ (1997) *J. Cell Biol.,* **139,** 1281-1292.
33. Lam M, Dubyak G, Chen L, Nunez G, Miesfeld RL, Distelhorst CW (1994) *Proc. Natl. Acad. Sci. U. S. A.,* **91,** 6569-6573.
34. Csordas G, Thomas AP, Hajnoczky G (1999) *EMBO J.*, **18,** 96-108.
35. He H, Lam M, McCormick TS, Distelhorst CW (1997) *J. Cell Biol.*, **138,** 1219-1228.
36. Kuo TH, Kim HR, Zhu L, Yu Y, Lin HM, Tsang W (1998) *Oncogene,* **17,** 1903-1910.
37. Murphy AN, Bredesen DE, Cortopassi G, Wang E, Fiskum G (1996) *Proc. Natl. Acad. Sci. U. S. A.,* **93,** 9893-9898.
38. Foyouzi-Youssefi R, Arnaudeau S, Borner C, Kelley WL, Tschopp J, Lew DP, Demaurex N, Krause KH (2000) *Proc. Natl. Acad. Sci. U. S. A.,* **97,** 5723-5728.
39. Ashkenazi A, Pai RC, Fong S, Leung S, Lawrence DA, Marsters SA, Blackie C, Chang L, McMurtrey AE, Hebert A et al (1999) *J. Clin. Invest.,* **104,** 155-162.
40. Ashkenazi, A (2002) *Nat Rev Cancer,* **2,** 420-430.
41. Green, DR (1998) *Cell,* **94,** 695-698.
42. Stegh AH, Barnhart BC, Volkland J, Algeciras-Schimnich A, Ke N, Reed JC, Peter ME (2002) *J. Biol. Chem.,* **277,** 4351-4360.
43. Li H, Zhu H, Xu C, Yuan J (1998) *Cell*, **94,** 491-501.
44. Luo X, Budihardjo I, Zou H, Slaughter C, Wang X (1998) *Cell*, **94,** 481-490.

45. Stegh AH, Herrmann H, Lampel S, Weisenberger D, Andra K, Seper M, Wiche G, Krammer PH, Peter ME. (2000) *Mol Cell Biol.*, **20,** 5665-5679.
46. Kagawa S, Gu J, Swisher SG, Ji L, Roth JA, Lai D, Stephens LC, Fang B (2000) *Cancer Res.*, **60,** 1157-1161.
47. Odero-Marah VA, Khalkhali-Ellis Z, Schneider GB, Seftor EA, Seftor RE, Koland JG, Hendrix MJ (2002) *Biochem Biophys Res Commun,* **295,** 800-805.
48. Sood AK, Fletcher MS, Gruman LM, Coffin JE, Jabbari S, Khalkhali-Ellis Z, Arbour N, Seftor EA, Hendrix MJC (2002) *Clin Cancer Res,* **8,** 2924-2932.
49. Harris C, Maroney AC, Johnson EM Jr (2002) *J Neurochem,* **83,** 992-1001.
50. Hay E, Lemonnier J, Fromigue O, Marie PJ (2001) *J Biol Chem,* **276,** 29028-29036.
51. Aguirre-Ghiso JA, Liu D, Mignatti A, Kovalski K, Ossowski L (2001) *Mol Biol Cell*, **12,** 863-879.
52. Aguirre-Ghiso JA, Estrada Y, Liu D, Ossowski L (2003) *Cancer Res*, **63,** 1684-1695.
53. Roth W, Reed JC (2002) *Nature Medicine,* **8,** 216-218.
54. Vitolo D, Zerbe T, Kanbour A, Dahl C, Herberman RB, Whiteside TL (1992) *Int J Cancer*, **51,** 573-580.
55. Silberstein, GB Tumour-stromal interactions. (2001) *Breast Cancer Res*, **3,** 218-223.
56. Rowley, DR (1998-9) *Cancer Metastasis Rev*, **17,** 411-419.
57. Tuxhorn JA, Ayala GE, Rowley DR (2001) *J Urol*, **166,** 2472-2483.
58. Li JJ, Colburn NH, Oberley LW (1998) *Carcinogenesis*, **19,** 833-839.
59. Liu, J, Yao, F, Wu, R, Morgan, M, Thorburn, A, Finley, RL. Jr, Chen, YQ (2002) *J. Biol. Chem,* **277,** 26281-26285.
60. Deng Y, Wu X (2000) *Proc. Natl. Acad. Sci. U. S. A.*, **97,** 12050-12055.

## FIGURES AND LEGENDS

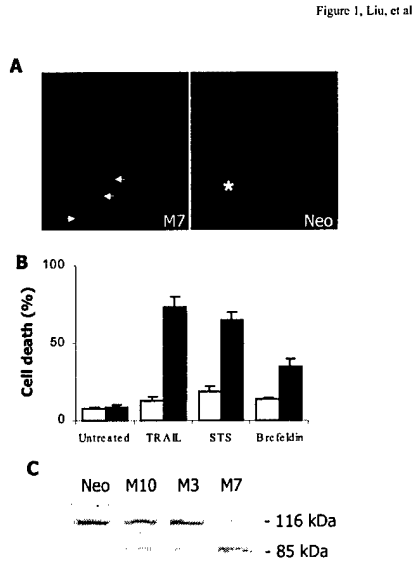


**Figure 1. Maspin Sensitizes Apoptotic Response of Prostate Carcinoma Cells to Distinct Stimuli.**
(A) Apoptotic nuclear morphology in STS-induced M7 and Neo cells. Nuclear DNA was stained with Hoechst (blue). White arrows indicate DNA condensation/fragmentation. Asterisk shows mitotic cells. X400. (B) Apoptosis induced by different stimuli in M7 (■) and Neo (□) cells. Cells were treated with TRAIL at 50 ng/ml for 1.5h, STS at 1 μM for 6 h, and brefeldin A at 30 μg/ml for 30 h. Apoptotic cells with fragmented nuclei as visualized by Hoechst staining were presented as a percentage of the total number of cells counted in the same field. Data shown are means of triplicate experiments; bars represent standard errors. (C) PARP cleavage in multiple maspin transfected clones (M3, M7, and M10) and Neo cells. Cells were treated with TNF-α (50 ng/ml)/CHX (2 μg/ml) for 3h. Whole cell extracts were loaded (50 μg per lane) for western blotting of PARP (116 kDa) and PARP-derived fragment (86 kDa).

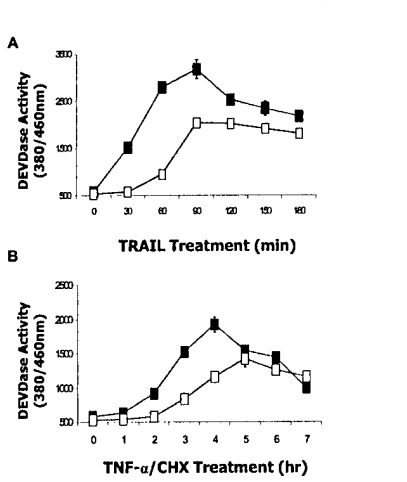


**Figure 2. Maspin Expression Leads to Increased Caspase-3 Activation.** M7 (■) and Neo (□) cells were treated with (A) TRAIL or (B) TNFα/CHX at the same dosage as described in Figure 1. A total of 30 μg cytosolic extracts prepared at the indicated time points was assayed for caspase-3 activity using fluorogenic Ac-DEVD-CMA as a substrate. The mean fluorescence productions obtained from triplicate repeats are used to represent caspase-3 activities. Bars represent standard errors.

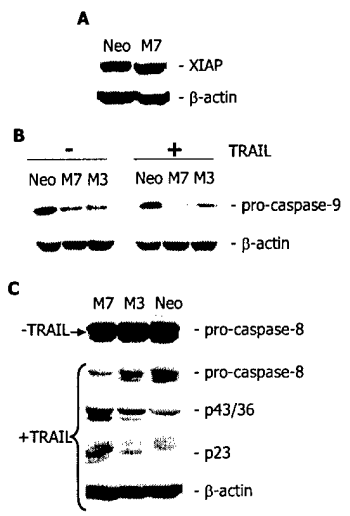


**Figure 3. Maspin Expression Has No Effect on XIAP, but Leads to Increased Cleavage of proaspase-8 and proaspase-9.** (A) Western blotting of XIAP using whole cell extracts from untreated M7 and Neo cells. (B) Western blotting of pro-caspase-9 using the whole cell extracts from M3, M7 and Neo cells that were either untreated or treated with TRAIL (50 ng/ml/50 min). (C) Western blotting of pro- and cleaved caspase-8 (p43/36 and p23) using the whole cell extracts from M3, M7 and Neo cells that were either untreated or treated with TRAIL (50 ng/ml/50 min). The western blots in A-C were reblotted with β-actin antibody, to normalize protein loading.

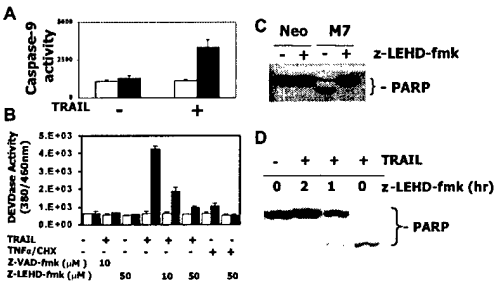


**Figure 4. The Predominant Executing Caspase in the Proapoptotic Effect of Maspin Is Caspase-9.** (A) The caspase-9 activity in M7 (■) and Neo (□) cells that were either untreated or treated with TRAIL (50 ng/ml/50 min). Thirty micrograms of cytosolic extract proteins from each sample were analyzed for caspase-9 activity using fluorogenic Ac-LEHD-CMA as a substrate. The relative enzymatic activities were obtained after subtracting the blank (without cell lysate proteins) from the total fluorescence productions. (B) The dose-dependent inhibition of the maspin effect by caspase-9 inhibitor. M7 (■) and Neo (□) cells were either untreated or treated with the indicated caspase inhibitors at the indicated final concentrations for 1 h prior to apoptosis induction by either TRAIL (50 ng/ml) for 50 min or TNF-α (50 ng/ml)/CHX (2 μg/ml) for 2.5 h. In the negative control experiments, caspase inhibitors were replaced with the same volume of DMSO, which was used to dissolve these compounds. The resulting cytosolic extracts were analyzed for caspase-3 activities using Ac-DEVD-CMA as a substrate. Fluorescence productions were reported as the relative enzyme activities. (C) PARP cleavage in M7 and Neo cells. Cells were either untreated or treated with 50 μM of caspase-9 inhibitor z-LEHD-fmk prior to apoptosis induction by TRAIL (50 ng/ml/50 min). (D) PARP cleavage in M7 cells that were treated with 50 μM of z-LEHD-fmk for indicated time periods prior to apoptosis induction by TRAIL (50 ng/ml/50 min). Cell extracts prepared from untreated M7 cells were used as a negative control.

In A and B, data represent the means of triplicate experiments. Bars represent standard errors. In C and D, whole cell extracts were loaded (50 μg per lane) for western blotting of PARP (116 kDa) and PARP-derived fragment (86 kDa).

Figure 5, Liu, et al

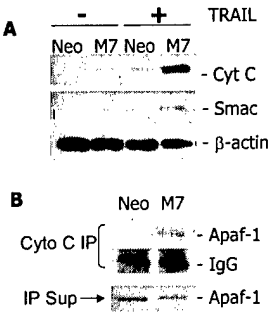


**Figure 5. The Mitochondrial Apoptotic Pathway Is Elevated in Maspin Transfected Cells.** (A) Immunodetection of Cytochrome c and Smac/DIABLO in cytosolic fractions of M7 and Neo cells that were either untreated or treated with TRAIL (50 ng/ml/50 min). Each sample contained 50 μg of protein. The western blot was stripped and reblotted with β-actin antibody to normalize the protein loading. (B) Association of Apaf-1 with Cytochrome c in cytosol. M7 and Neo cells were both treated with TRAIL (50 ng/ml/50 min) prior to the preparation of the cytosolic fractions. A total of 300 μg of cytosolic proteins were used for IP. The resulting immunoprecipitated proteins by Cytochrome c antibody, as well as the supernatants derived from the IP reactions (50 μg/lane) were analyzed by western blotting for Apaf-1. Cytochrome c IgG in the immunoprecipitate fractions, detected by the secondary antibody in western blotting, serves as a loading control.

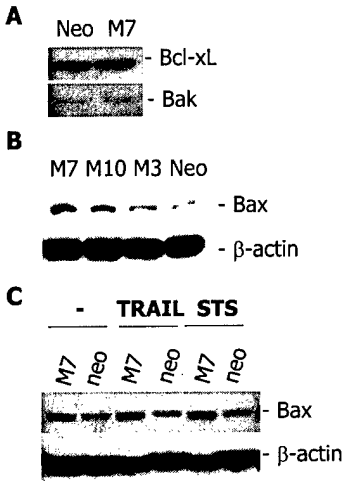


**Figure 6. Bax Is Up-regulated in Maspin Transfected Cells.** (A) Western blotting of Bcl-xl and Bak using whole cell extracts prepared from untreated M7 and Neo cells. (B) Western blotting of Bax using whole cell extracts prepared from untreated M3, M7, M10 and Neo cells. (C) Western blotting of Bax in the whole cell extracts of M7 and Neo cells that were either untreated, TRAIL-treated, or STS-treated. In A-C, 50 μg of cell extract proteins were loaded to each lane. The western blots in B and C were stripped and reblotted with β-actin antibody to normalize the protein loading.

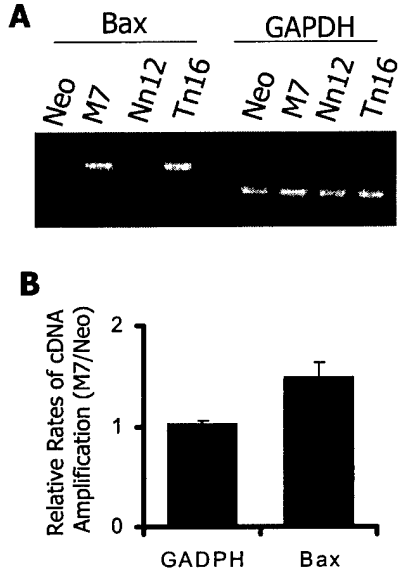


**Figure 7. The Bax Up-regulation in Maspin Transfected Cells Is Transcriptionally Regulated.** (A) Semi-quantitative RT-PCR detection of Bax mRNA using the total RNA from M7 and Neo cells, as well as Tn16 and Nn12 cells. Parallel RT-PCR with GAPDH-specific primers was performed using the same set of RNA samples to normalize the equal loading. (B) Real-time PCR quantification of Bax mRNA using the total RNA prepared from M7 and Neo cells. Fluorescence productions derived from SYBR Green labeling of PCR products are expressed as fold increase of M7/neo at the end of the cycle immediately after the slower reaction in the pairs reached the cycle threshold. Parallel Real-time RT-PCR with GAPDH-specific primers was performed to normalize the equal loading. Data represent means of independent experiments with two different RT-PCR machines. Each experiment was performed in quadruple repeats. Bars represent standard errors.

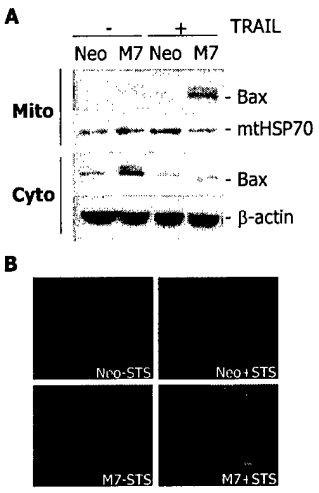


**Figure 8. Bax in Maspin Transfected Cells Is Effectively Translocated to Mitochondria in Response to Apoptosis Induction.** (A) Western blotting of Bax in the cytosolic and mitochondrial fractions prepared from M7 and Neo cells that were either untreated or treated with TRAIL (50 ng/ml/50 min). A total of 50 μg of protein was loaded to each lane. Western blotting of β-actin and mtHSP70 were used to normalize the loading of cytosolic proteins and mitochondrial proteins, respectively. (B) Immunofluorescent Staining of Bax. Cells either untreated or treated with STS (1 μM/3h) were subjected to immunofluorescent staining using polyclonal antibody against Bax as the primary antibody. The secondary antibody was Goat-anti-rabbit IgG conjugated with Oregon Green. The confocal fluorescent images were acquired using a Zeiss LSM 310 microscope. X400.

**PART III**

Our unexpected results prompted a new investigation of the role of maspin in breast tumor progression. To further explore the clinical application of maspin in human cancer, it is critical to understand the in vivo biological function of maspin in tumor progression. To this end, ne of the most powerful models used to examine multistage carcinogenesis has been MMTV/TGF-α transgenic mouse. Elevated levels of TGF-α have been detected in transformed keratinocytes and in a variety of naturally occurring human tumor types (Gottlieb, 1988; Reddy, 1994). In addition, the role of TGF-α in neoplasia has been confirmed in a variety of experimental systems, including transgenic mice in which initially hyperplasia and later neoplasia of liver and mammary glands were observed (Jhappan, 1990; Matsui, 1990; Sandgren, 1990). In collaboration with Dr. Kaladhar Reddy at WSU, we evaluated the role of maspin as a tumor suppressor using MMTV/TGF-α transgenic mouse model. This results have been published on Oncogene (2000)

**Maspin Expression Inversely Correlates with Breast Tumor Progression in MMTV/TGF-alpha Transgenic Mouse Model**

Kaladhar B. Reddy, Richard McGowen, Lucia Schuger, Daniel Visscher and Shijie Sheng

ABSTRACT

Maspin is a novel serine protease inhibitor (serpin) with tumor suppressive activity. To date, despite the mounting evidence implicating the potential diagnostic/prognostic and therapeutic value of maspin in breast and prostate carcinoma, the lack of a suitable animal model hampers the in vivo investigation on the role of maspin at different stages of tumor progression. In this study, we used MMTV/TGF-α transgenic mouse model to study the expression profile of maspin in mammary tumor progression. Histopathological examinations of MMTV/TGF-α transgenic mice revealed TGF-α expression leading to hyperproliferation, hyperplasia, and occasional carcinoma in mammary gland. Interestingly, when MMTV/TGF-α transgenic mice were breed to homozygocity, they also developed characteristic skin papillomas. Immunohistochemistry analysis of maspin expression in the breast tissues of TGF-α transgenic mice showed a direct correlation between down-regulation of maspin expression and tumor progression. The loss of maspin expression was concomitant with the critical transition from carcinoma in situ to invasive carcinoma. Subsequent in-situ hybridization analyses suggest that the down-regulation of maspin expression is primarily a transcriptional event. This data is consistent with the tumor suppressive role of maspin. Furthermore, our data suggests that MMTV/TGF-α transgenic mouse model is advantageous for *in vivo* evaluation of both the expression and the biological function of maspin during the slow mutli-stage carcinogenesis of mammary gland.

INTRODUCTION

Maspin is a novel serine protease inhibitor (serpin) initially identified in normal mammary epithelial cells (Zou, 1994). Several subsequent studies have confirmed the down-regulation of maspin in invasive breast carcinoma and breast tumor metastases, as well as in an array of established breast carcinoma cell lines (Zou, 1994), (Sager, 1994). *In vitro* analyses suggest that the expression of maspin may be tightly regulated by a complex mechanism at the transcriptional level. Recent work by Zou et al. revealed a direct activation of maspin expression by the tumor suppressor gene p53 in both prostatic and mammary carcinoma cell lines, suggesting a role of maspin in p53-mediated tumor suppression (Zou, 2000). Further biological studies have shown that recombinant maspin inhibits the motility and invasion of both breast and prostate carcinoma cell lines *in vitro* (Sheng, 1994), (Sheng, 1996). Biochemical evidence suggests that maspin act as a potent inhibitor of surface-bound tissue type plasminogen

activator (tPA) (Sheng, 1998) and cell-associated urokinase type plasminogen activator (McGowen, 2000). Given the important role of proteolysis during tumor cell migration and invasion, it is likely that maspin inhibits tumor cell motility and invasion, at least in part by inhibiting the paracellular plasminogen activation.

To further explore the clinical application of maspin in human cancer, it is critical to understand the in vivo biological function of maspin in tumor progression. To this end several animal models have been used in previous studies. For example, endogenous expression of maspin inhibits the growth and metastasis of orthotopic breast tumor xenograft in nude mice (Zou, 1994), (Sager, 1994). Recombinant maspin-GST fusion protein was shown to block the angiogenesis induced by subcutaneous prostatic tumor xenograft in nude mice (Zhang, 2000). In addition, an earlier study by Zhang et al showed that mammary specific maspin overexpression in transgenic mice severely disrupted the mammary gland development, possibly by preventing cell migration (Zhang, 1997). While these *in vivo* data provide valuable insight into the biological function of maspin at different pathophysiological stages of the mammary gland, none of those animal models is suitable for a detailed assessment of the regulation as well as the role of maspin in the entire course of breast carcinogenesis *in vivo*.

One of the most powerful models used to examine multistage carcinogenesis has been MMTV/TGF-α transgenic mouse. Elevated levels of TGF-α have been detected in transformed keratinocytes and in a variety of naturally occurring human tumor types (Reddy, 1994), (Gottlieb, 1988). In addition, the role of TGF-α in neoplasia has been confirmed in a variety of experimental systems, including transgenic mice in which initially hyperplasia and later neoplasia of liver and mammary glands were observed (Sandgren, 1990), (Jhappan, 1990), (Matsui, 1990).

TGF-α is a 50 amino acid 5.6 kDa secreted polypeptide that is cleaved from a large integral membrane glycoprotein. The matured TGF-α molecule shares 35% sequence homology with epidermal growth factor (EGF), binds to the same receptor, and has similar biologic effects (Derynck, 1988). A commonly cited action of both TGF-α and EGF is that they act as potent mitogens in a number of epithelial cell systems (Carpenter, 1979). The transgenic studies further demonstrated a proliferative role for TGF-α in the development of mammary neoplasia, cooperating with c-myc/TGF-α and Neu oncogenes (Lenferink, 2000), (Rose-Hellekart, 2000). On the other hand, inhibitory and modulating agents of the EGFR signaling pathways such as anti-EGFR antibodies and specific protein kinase inhibitors have been shown to prevent the development of TGF-α-induced neoplasia and tumor formation (Lenferink, 2000), (Rose-Hellekart, 2000).

In this study, we evaluated the role of maspin as a tumor suppressor using MMTV/TGF-α transgenic mouse model, which show a range of abnormalities in the mammary gland including lobular hyperplasia, adenomas, hyperkeratosis and mammary carcinoma. Using a combination of immunohistochemistry and *in situ* hybridization, we show that both normal myoepithelial cells and normal ductal epithelial cells express maspin at a high level. Hyperplastic mammary epithelium and mammary carcinoma in situ (DCIS) expressed a moderate level of maspin. However more malignant stage of tumors such as invasive carcinoma show a significant reduction or total loss of maspin. Taken collectively, the inherent multi-stage nature of breast carcinogenesis in TGF-α transgenic mice provided us a valuable system to assess the level of maspin in different stages of tumor progression in the same tumor such as hyperplasia (ductal or lobular), carcinoma in situ, or invasive carcinoma.

## MATERIALS AND METHODS

Generation and Characterization of MMTV/TGF-α Transgenic mice. The construction of MMTV LTR was similar to the previously published work of Matsui (Matsui, 1990). In brief, pMMTV/TGF-α, the SV40 early promoter region in the vector pKCR was replaced by the complete MMTV-LTR. A 925 bp

human TGF-α cDNA (kindly provided by Dr. Bell, University of Chicago) was then inserted into EcoRI site of β-glonin exon 3. The 3.6 kb XhoI fragment was purified and microinjected into (C57BL X DBA) fertilized eggs. Homozygous TGF-α transgenic mice were obtained by breeding two heterozygous TGF-α transgenic mice. For histological examination of the mammary glands, the skin containing the mammary fat pads was fixed in 10% buffered formalin for at least 24 h. and then embedded in paraffin. Routinely, 5 μm sections of the whole mount tumor and mammary tissue were stained with hematoxylin and eosin using a standard protocol.

RNase Protection Assay. To confirm the expression of the TGF-α transgene, RNase protection assay was performed as described previously (Reddy, 1994). Briefly, the TGF-α probe used for RNase protection analysis was 152-bp SphI-ApaI fragment cloned in antisense orientation into pGEM7zf (provided by Dr. Kern, Lombardi Cancer Center, Washington, DC). The resulting plasmid was linearized with BamHI and transcribed with T7 polymerase in the presence of $^{32}$P-labeled ATP. Thirty micrograms of total RNA from each sample were hybridized overnight at 50 °C with 50,000 cpm of probe in 30 μl of buffer containing 80% formamide, 40 mM piperazine-N,N'-bis(2-ethanesulfonic acid), 0.4 M NaCl, and 0.1 M EDTA. Samples were subsequently digested with 40 μg/ml RNase A (Sigma) for 30 min at 25 °C. Digestion was terminated with proteinase K and SDS. The samples were pelleted and resuspended in 5 μl of an 80% formamide loading buffer and run on 6% polyacrylamide sequencing gel with 8 M urea. Size markers were prepared by end labeling MspI-digested fragments of pBR322. The gels were dried and exposed to X-ray film in the presence of an intensifying screen at –70 °C for 1 or 2 days.

Immunohistochemistry. The expression of maspin protein was immunostained by using AbS4A, a polyclonal antibody raised against the unique reactive loop sequence of maspin (Zou, 1994), on 5-μm sections cut from the aforementioned tissue blocks. The immunohistochemical staining was performed at room temperature unless otherwise stated for a specific step. The slides were deparaffinized in xylene and rehydrated in graded ethanols to PBS. Endogenous peroxidase activity was destroyed by treating the tissue for 10 minutes in 1% $H_2O_2$ in methanol. Antigen was retrieved in 10mM sodium citrate (pH 6.0) by microwave heating for 3 minutes in the case of surgical specimens and for 5 minutes on the whole mount autopsy tissues. Following the initial blocking with 10% normal goat serum for 30 minutes, the primary antibody was applied at 4.0 μg/ml with 1% BSA and 0.01% Triton-X100 and allowed to incubate overnight at 4°C. The tissues were then blotted with biotinylated anti-rabbit secondary antibody (Zymed) for 30 minutes, and subsequently with strepavidin-HRP (Zymed). The DAB color reaction was employed for detection according to the manufacturer's directions (Vector). The slides were counterstained with hematoxylin and dehydrated in a series of graded ethanols and xylene followed by mounting with Permount (Fisher). The negative controls of immunohistochemical staining were performed in the similar fashion except that purified preimmune IgG at a final concentration of 4 μg/ml was used in the place of Abs4A.

In-situ hybridization: The PCR-amplified full length coding sequence of maspin cDNA in the pGEM7Zf(+) vector (Xia, 2000) was used as the template for in vitro transcription with the DIG labeling kit (from Boehringer Mannheim, Indianapolis, IN). The resulting labeled full-length maspin mRNA was hydrolyzed to approximately 0.2 kb fragment, then used in the subsequent in situ-hybridization procedure. The DIG-labeled full-length sense strand maspin mRNA was used in parallel as the negative controls.

The in situ hybridization was performed as described by the manufacturer with some modifications. Briefly, tissue specimens were deparaffinized in xylene and rehydrated through a series of graded ethanols to PBS. Following the permeabilization with 25μg Proteinase K in Tris/EDTA buffer (pH 8.0)

for 30 minutes at 37 °C, the specimens were denatured with 4X SCC in 50% deionized formamide at 37°C for 10 minutes. The slides were then hybridized with 5-10 ng of DIG labeled probe overnight at 60 °C, followed by two washes with 0.1X SCC at 60 °C (with agitation). The specifically bound DIG-labeled DNA was detected by the color reaction of the horse-radish peroxidase-conjugated anti-DIG antibody. The sections are then counter stained with methyl green and mounted with Permount.

RESULTS

Incidence of Sporadic Mammary Carcinoma Is Increased in MMTV/TGF-α Transgenic Mice. Homozygous TGF-α transgenic mice were identified by southern blot analysis of tail DNA, and by 100% transmission of the gene when bread with non-transgenic mice (data not shown). In transgenic mice, TGF-α RNA expression was confirmed by RNase protection analyses. High levels of TGF-α expression were seen in mammary gland and a relatively low level of TGF-α was detected in sebaceous glands and lungs of transgenic multiparous females (Fig. 1). In contrast, age-matched non-transgenic multiparous females exhibited low levels of TGF-α expression in mammary glands and no signal in sebaceous gland and lung.

The mammary glands from transgenic or nontransgenic virgin females mice (4 weeks) showed no alveolar development. While the non-transgenic mice were not symptomatic throughout their lives, all 50 female transgenic mice used showed significant breast hyperplasia after multiple pregnancies. Twelve of these transgenic mice developed hyperkeratosis and bilateral lumps in their mammary glands. Histologic examination of whole mount tissues revealed significant alveolar hyperplasia throughout the entire mammary glands in the transgenic but not in nontransgenic mice (data not shown). Histologic examination revealed that some of the TGF-α- induced mammary tumors developed breast and sebaceous gland carcinoma as shown in Figure 2. Although these transgenic mice did no have distal metastases, five of them developed invasive breast carcinoma at 6-8 months of age, as shown in Figure 3.

Maspin Expression Inversely Correlates with the Mammary Tumor Progression in MMTV/TGF-α Transgenic Mice. In transgenic mouse group, each tumor specimen had multiple regions of hyperplasia and carcinoma *in situ*. Since the mammary tumors developed are rather small in size, it is very difficult to extract sufficient amount of either protein or RNA for quantitative comparison of maspin expression at a gross level by immunoblotting or Northern blotting. To investigate the expression and the localization of maspin protein in mouse breast tumor progression, we performed semi-quantitative immunohistochemical staining on the whole mount mammary tissues from 5 MMTV/TGF-α transgenic mice and 2 age-matched nontransgenic mice. Figure 2 shows representative immunohistochemical staining results. As can be seen, the oligopeptide-derived polyclonal antibody against maspin, Abs4A, exhibited a specific immunoreactivity with normal myoepithelial cells and normal luminal epithelial cells (Figure 2B). The parallel immunostaining with the preimmune serum gave rise to a negative staining pattern (Figure 2A). Furthermore, maspin expression appeared to be cytoplasmic in mammary epithelial cells and was not found in the stroma. As compared to normal mammary epithelium, mammary hyperplasia exhibited a moderate level of maspin expression (Figure 2C), while mammary carcinoma cells showed little or no maspin immunoreactivity (Figure 2D arrow). Microscopic examination using a higher magnification indicated that the loss of maspin expression was associated with invasive mammary carcinoma (Figure 3B). In all tumor samples from the transgenic group (5/5), consistent differential expression of maspin was observed.

To address whether maspin was specifically produced by mammary epithelial cells and whether maspin was differentially expressed at the mRNA level, in-situ hybridization was performed with the whole mount mammary tissues. While the sense-strand of maspin cDNA did not give rise to detectable

signal (data not shown), a strong positive staining of maspin mRNA was detected in benign luminal and the myoepithelial cells (Figure 4A). Hyperplastic mammary epithelium featured heterogeneous maspin staining of a moderate intensity (Figure 4B). Mammary carcinoma in situ and invasive carcinoma cells expressed little or no maspin mRNA (Figure 4C). The stroma of both transgenic and non-transgenic mouse mammary glands was free of maspin mRNA signal.

DISCUSSION

We showed that TGF-α overexpression in adult transgenic mice induced hyperproliferation, hyperplasia, and occasional carcinoma in mammary gland. Both immunohistochemistry and *in situ* hybridization analyses demonstrated a down-regulation of maspin expression in the mouse mammary tumor progression. Our data is consistent with the previous finding that maspin expression is down-regulated in human breast carcinoma and further support a tumor suppressive role of maspin. In view of several remaining critical issues, the MMTV/TGF-α transgenic mouse model offers the following unique advantages.

The MMTV/TGF-α transgenic model is of choice for studying the *in vivo* expression profile and regulation of maspin in mammary tumor progression. We showed that overexpression of TGF-α is not sufficient to cause the malignant phenotype. It is conceivable that complex secondary events are needed in the development of the heterogeneous multi-stage mammary neoplasia. Thus, MMTV/TGF-α transgenic mouse model is likely to provide a broad spectrum of pathological changes similar to those involved in naturally occurring human breast cancer. Compared to the tumor xenograft mouse models that have been successfully used to evaluate the effect of maspin in tumor intervention, MMTV/TGF-α transgenic mice undergo slower multi-stage carcinogenesis, thus may be a unique tool for testing the potential application of maspin in tumor prevention as well as the diagnostic/prognostic value of maspin as a molecular marker.

Since maspin is abundantly expression in the normal mammary epithelial cells both in the nontrnasgenic and the MMTV/TGF-α transgenic mice, it is unlikely that TGF-α directly activates or inactivates the maspin transcription. It been noted that maspin expressed in normal human mammary gland is primarily co-localized with myoepithelial cells (Zou, 1994), (Sternlicht, 1997). Sternlicht et al hypothesized that myoepithelial cells are a natural defense against malignancy (Sternlicht, 1997). Interestingly, in mouse mammary gland, both luminal epithelial cells and myoepithelial cells showed strong immunoreactivity with the maspin antibody (Figure 2) and were tested positive for maspin mRNA (Figure 4). It remains to be determined whether the luminal epithelial cells in mouse mammary gland are subject to the same regulation as in human mammary gland. Nonetheless, mammary carcinoma *in situ* of both human (Zou, 1994) and mouse origin (Figure 2, 4) show a reduced level of maspin expression. Furthermore, in both human (Zou, 1994) and mouse (Figure 3), the loss of maspin expression correlates with the transition to invasive carcinoma. These data suggest that the molecular mechanisms underlying the differential expression of maspin in human and mouse are similar.

Previous *in vitro* promoter activity analyses indicate that p53 directly activates the transcription of maspin (Zou, 2000). Our current evidence that maspin expression is differentially regulated in TGF-α induced mammary carcinogenesis opens a new window of possibilities regarding the upstream molecular pathways that regulate maspin expression. In particular, we showed that MMTV/TGF-α transgenic mice expressed maspin in normal and premalignant mammary epithelial cells, but lost maspin expression at the transition from noninvasive tumor to invasive breast carcinoma. It is thought that TGF-α exerts its stimulatory effect on mitosis by activating the tyrosine kinase activity of the epidermal growth factor receptor (EGFR) (Humphreys, 2000). Interestingly, several recent studies suggest that TGF-α induced tumorigenecity may directly involve p53. The elegant studies of Wagner et al and Lin et

al suggest that TGF-α overexpression may lead to a transient up-regulation of p53 via the *ras* oncogene, and subsequently lead to the loss of p53 due to genetic instability prior to malignancy (Wagner, 2001), (Lin, 2001). Taken together, it is possible that the differential expression of maspin in TGF-α induced mammary carcinogenesis is regulated, at least in part, by p53 at this critical stage of tumor progression.

It is important to point out that since several *in vitro* studies also suggest that maspin expression may be hormonally regulated (Zhang, 1997), (Yamada, 2000), the transcriptional regulation of maspin expression may be more complex. Future hypothesis-driven analyses using both TGF-α transgenic mice and human tissue specimens need to be conducted in parallel with in vitro promoter activity analyses in order to evaluate the roles of candidate regulating molecules in maspin transcriptional. In addition, to better assess the biological significance of maspin in breast tumor progression, the correlation of maspin with other molecular markers of breast cancer such as estrogen receptor (ER), HER2 and p53 need to be established.

The MMTV/TGF-α transgenic mouse model may also facilitate the elucidation of the molecular mechanism of maspin. Accumulated evidence supports a role of maspin as an inhibitor of tumor invasion. At the molecular level, it has been shown that maspin specifically inhibits bound-plasminogen activators (both tissue-type and urokinase-type) (Sheng, 1998), (McGowen, 2000). Thus, it is hypothesized that maspin inhibits tumor cell invasion by inhibiting the plasminogen activator-mediated proteolysis. By crossing various genetically modified mice, one can test *in vivo* functional interaction between maspin and plasminogen activator(s). In parallel, the MMTV/TGF-α transgenic model could be used to evaluate whether the expression of maspin is correlated with that of its candidate target molecules such as urokinase-type plasminogen activator (uPA) in the natural tumor progression.

In conclusion, we found a direct correlation between down-regulation of maspin expression and the stage of mammary tumors in MMTV/TGF-*a* transgenic mice. Our data suggests that MMTV/TGF-α transgenic mouse model is advantageous for *in vivo* evaluation of both the expression and the biological function of maspin during the slow mutli-stage carcinogenesis of mammary gland.

ACKNOWLEDGEMENTS

This work was supported in part by a Prostate Cancer Pilot Grant from National Cancer Institute/Wayne State University CA69845 (to S. S.), a Ruth Sager Memorial Fund established by Dr. Arthur B. Pardee (to S. S.), and by NIH grants CA 64248 and CA 83964 (to K. B. R.).

REFERENCES

Carpenter, G., Cohen, S. (1979). *Annu. Rev. Biochem.*, 48, 193-216.

Derynck, R. (1988). *Cell*, 54, 593-595.

Gottlieb, A.B., Chang, C. K., Posnett, D. N., Fanelli, B., Tam, J. P. (1988). *J. Exp. Med.*, 167, 670-675.

Humphreys, R.C., Hennighausen, L. (2000). *Oncogene*, 19, 1085-1091.

Jhappan, C., Stahle, C., Harkins, R. N., Fausto, N., Smith, G. H., Merlino, G. T. (1990,). *Cell*, 61, 1137-1146.

Lenferink, A.E.G., Simpson, J. F., Shawver, L. K., Coffey, R. J., Forbes, J. T., Arteaga, C. L. (2000). *Proc. Natl. Acad. Sci. USA*, 97, 9609-9614.

Lin, A.W., Lowe, S. W. (2001). *Proc Natl Acad Sci U S A*, 98, 5025-5030.

Matsui, Y., Halter, S. A., Holt, J. T., Hogan, B. L., Coffey, R. J. (1990,). *Cell*, 61, 1147-1155.

McGowen, R., Biliran, H. Jr., Sager, R., and Sheng, S. (2000). *Cancer Res.*, 60, 4771-4778.

Reddy, K.B., Yee, D., Hilsenbeck, S. G., Coffey, R. J., Osborne, C. K. (1994). *Cell Growth Differ.*, 5, 1275-1982.

Rose-Hellekart, T.A., Sandgren, E. P. (2000). *Oncogene*, 19, 1092-1096.

Sager, R., Sheng, S., Anisowicz, A., Sotiropoulou, G., Zou, Z., Stemman, G., Swisshelm, K., Chen, Z., Hendrix, M. J. C., Pemberton, P., Rafidi, K., and Ryan, K. (1994). *Cold Spring Harbor Symposium on Quantitative Biology*, Vol. LIX, pp. 537-546.
Sandgren, E.P., Luetteke, N. C., Palmiter, R. D., Brinster, R. L., Lee, D. C. (1990). *Cell*, 61, 1121-1135.
Sheng, S., Carey, J., Seftor, E., Dias, L., Hendrix, M. J. C., and Sager, R. (1996). *Proc. Natl. Acad. Sci. USA* . 93, 11669-11674.
Sheng, S., Pemberton, P., and Sager, R. (1994). *J. Biol. Chem.*. 269, 30988-30993.
Sheng, S., Truong, B., Frederickson, D., Wu, R., Pardee, A. B., and Sager, R. (1998). *Proc. Natl. Acad. Sci. U.S.A.*, 95, 499-504.
Sternlicht, M.D., Kedeshian, P., Shao, Z. M., Safarians, S., Barsky, S. H. (1997). *Clin. Cancer Res.*, 3, 1949-1958.
Wagner, M., Greten. F. R., Weber, C. K., Koschnick, S., Mattfeldt, T., Deppert, W., Kern, H., Adler, G., Schmid, R. M. (2001). *Gene and Dev.*, 15, 286-293.
Xia, W., Lau, Y. K., Hu, M. C., Li, L., Johnston, D. A., Sheng, S., El-Naggar, A., and Hung, M. C. (2000). *Oncogene*, 19, 2398-2403.
Yamada, N., Tamai, Y., Miyamoto, H., and Nozaki, M. (2000). *Gene*, 11, 267-274.
Zhang, M., Magit, D. and Sager, R. (1997). *Proc. Natl. Acad. Sci. USA*, 94, 5673-5678.
Zhang, M., Sheng, S., Mass, N., and Sager, R. (1997,). *Mol. Med*, 3, 49-59.
Zhang, M., Volpert, O., Shi, Y. H., and Bouch, N. (2000). *Nat. Med.*, 6, 196-199.
Zou, Z., Anisowicz, A., Hendrix, M. J. C., Thor, A., Neveu, M., Sheng, S., Radfidi, K., Seftor, E., and Sager, R. (1994). *Science*, 263, 536-529.
Zou, Z., Gao, C., Nagaich, A. K., Connell, T., Saito, S., Moul, J. W., Seth, P., Appella, E., and Srivastava, S. (2000). *J. Biol. Chem.*. 275, 6051-6054.

FIGURES AND LEGENDS

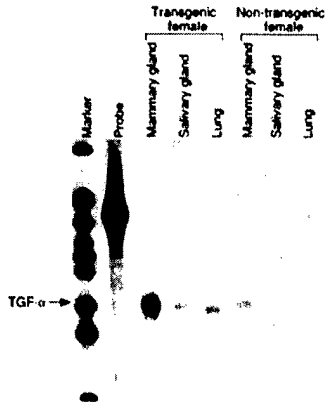


Figure 1. Targeted Expression of TGF-a in MMTV/TGF-α Transgenic Mice
Ribonuclease Protection Analysis of TGF-α transgene expression in various mouse tissues. Total RNA from mouse tissues was hybridized to uniformly labeled TGF-α probe, subjected to RNase digestion, electrophoresed in denaturing polyacrylamide gel, and exposed to autoradiographic film. The detected band was a fragment of TGF-α transgene.


Figure 2. Immunohistochemical Staining of Maspin in the Mammary Gland of MMTV/TGF-α Transgenic Mice.
(A): Immunohistochemical staining of the nontransgenic mouse mammary tissue using the preimmune se the high level expression of maspin in normal luminal and myoepithelial cells. (C): the moderate expression of n hyperplastic mammary epithelial cells; (D): down-regulation of maspin in mammary carcinoma. The reddish bro represents positive maspin immunoreactivity. The cell nuclei are counter-stained blue. The white arrow in (D) mammary carcinoma.

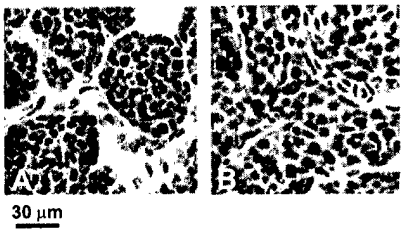


Figure 3. Maspin Expression Is Down-regulated in Invasive Mammary Carcinoma.
Microscopic examination at higher magnification shows maspin present in mammary carcinoma in situ (A), but lost in invasive mammary carcinoma (B) of TGF-α transgenic mice. Maspin detected by immunohistochemical staining gives rise to the reddish brown-color. The cell nuclei are counter-stained blue.

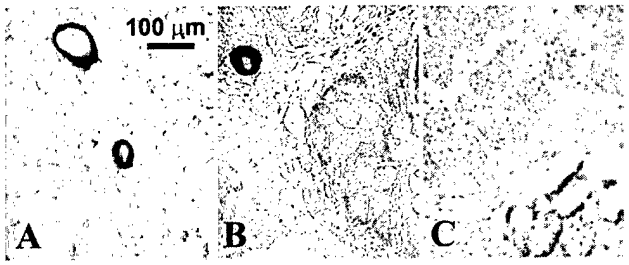


Figure 4. *In-situ* Hybridization for maspin mRNA in the Mammary Glands of TGF-α Transgenic Mice. The purplish blue color represents the positive detection of maspin mRNA. The light green colored spheroids are the counter-stained nuclei. (A): benign mammary epithelium with marked maspin mRNA; (B) reduced level of maspin mRNA in hyperplastic mammary epithelium; (C) the low expression of maspin mRNA in mammary carcinoma.

## PART IV: OTHER IMPORTANT RESULTS FROM DOD-SUPPORTED RESEARCH

### Maspin Inhibits Cell Detachment

Previously we have shown that maspin inhibits breast tumor cell motility and invasion. Subsequently, in collaboration with Dr. May Hendrix's laboratory, we showed that endogenous expression of msapin in MDA-MB-435 cells induced a more differentialted phenotype which correlated with a marginally increased cell adhesion to Fibronectin substratum. Considering that cell migration involves the concerted actions of cell adhesion (at the lamellapodia extension) and cell detachment (at the rare ends). We also examined the effect of maspin on cell detachment. As shown in Figure 1, MDA-MB-435 cells seeded on various ECM components (for 6 hours) followed by a Calcium-withdrawal induced cell detachment for 30 minutes at room temperature. The remaining attached cells were counted using a Coulter Counter. Maspin dramatically inhibited cell detachment from matrigel matrix, collagen type I, collagen type IV, laminin, fibronectin, and vitronectin.

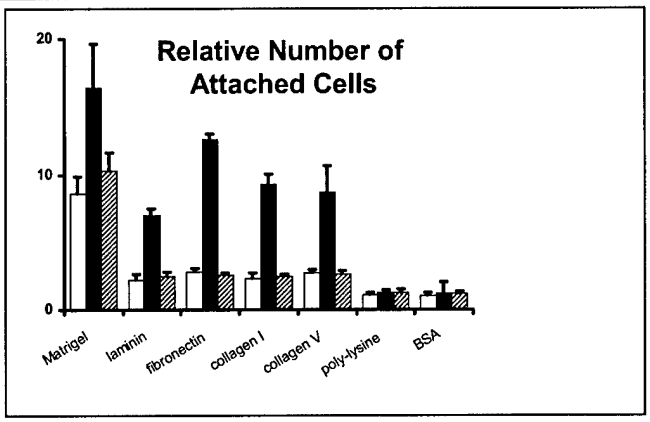


**Figure 1. rMaspin inhibits cell detachment from the established cell-matrix contacts to various ECM components.** Cells were seeded on the culture dishes precoated with the indicated ECM components. Cells were then cultured for 6 hours and then forced to detached by a balanced salt solution that had been depleted of Calcium). (□) untreated cells; (■) rMaspin at 20 μg/ml; (▨) chick ovalbumin at 20 μg/ml. The number of cells remaining after the detachment was normalized by the results with untreated seeded on BSA coated plates.

Thus, maspin may inhibit tumor invasion and motility at the step of cell detachment. Furthermore, the maspin effect did not appear to be specific for any particular ECM components, we hypothesized that maspin may inhibit a common step in cell detachment. At this time, my laboratory had shown that, in deed, maspin (both endogenously expressed or purified recombinant protein) specifically inhibited the prostate tumor cell surface-associated uPA activity. uPA is a serine protease and can converts plasminogen to plasmin. Accumulated evidence suggests that uPA/plasmin is a powerful proteolytic cascade, capable of ECM degradation and activating other ECM-degrading enzymes such as MT1-MMP and MMP-9. To test whether the maspin effect on cell detachment was a result of pericellular proteolytic inhibition, recombinant maspin was tested in MDA-MB-435 cells-mediated ECM degradation. ECM deposited by endothelial cells were metabolic labeled with $^{3}H$ (with $^{3}H$-labeled methionine and cysteine in the serum-free medium). MDA-MB-435 cells were added to the labeled ECM and continuously cultured at 37 °C. Degraded ECM components that were released to the culture medium were collected and counted. As shown in Figure 2, purified recombinant maspin added at 20 μg/ml (and replenished every 12 hours) significantly inhibited MDA-MB-435 cells mediated ECM degradation. The inhibitory effect of maspin was dose-dependently reversed by the polyclonal antibody made against maspin reactive site loop sequence, Abs4A. This evidence indicates that maspin acts as a protease inhibitor and its reactive site loop sequence play a critical role in inhibiting proteolysis-mediated ECM degradation.

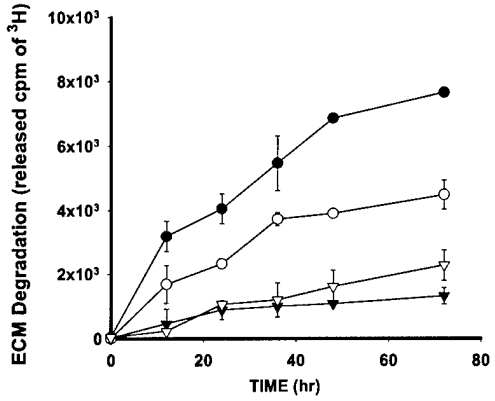


**Figure 2. rMaspin Inhibits MDA-MB-435 cells mediated ECM degradation.** $^3$H-labeled extracellular matrix deposited by endothelial cells were degraded by recombinant maspin. The inhibitory effect of maspin on MDA-MB-435 mediated ECM degradation was reversed in a dose-dependent manner by maspin specific antibody Abs4A. The ECM degradation is presented by the released ECM fragments that could be measured by radioactivity counting. Each point represents the average of three repeats and the error bards represents the standard error. (●) Untreated control; (▼) rMaspin 20 μg/ml; (▽) rMaspin 20 μg/ml plus 5 μg/ml of Abs4A; (O) rMaspin 20 μg/ml plus 20 μg/ml of Abs4A

## Generation and Characterization of Additional Maspin Mutants

Current evidence supports the role of maspin as a serine proteinase inhibitor. The primary protein sequence and the predicted general structural framework of maspin are similar to those of the inhibitory serpins and are consistent with the functional evidence that the tumor suppressive activity of maspin depends on its intact RSL. To elucidate the structural-functional relationship of maspin, three maspin mutants have been successfully overexpressed using a baculo-virus expression system (Pharmingen). Modified heparin column chromatography procedures were developed to purify these maspin variants (Figure 3).

Two mutants of maspin made in the second year of this project: maspinR330A and maspin/KDEL mutant were tested in cell detachment assay. As shown in Figure 4, while the wild type maspin protects MDA-MB-435 cells from Calcium withdrawal-induced detachment, these two mutants did not prevent the cell detachment. These results further demonstrate the essential role of msapin reactive site loop sequence in its inhibitory activityon pericellualr proteolysis.

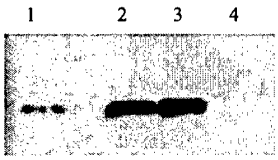


Figure 3. Expression and Purification of Maspin and Maspin-derivatives
(A): schematic structures of three maspin-derived polypeptides; (B): Western blot of maspin and maspin-derivatives expressed by baculo virus-infected *Sf*9 insect cells. Lanes 1-4 are the lysates of cells expressing wild type Maspin, Maspin(R330A), Maspin (ΔCT329), and Maspin(ΔCT315), respectively. Lanes1 and 2 were detected by Abs4A, while lanes 3 and 4 were detected by a polyclonal antibody against recombinant wild type maspin (Pharmingen). (C): Purification of maspin by heparin-affinity chromatography followed by Coomassie blue stained SDS-PAGE. Lane 1 is the lysate of uninfected insect cells . Lane 2 is the lysate of Sf9 cells infected with maspin-expressing baculo virus. Lane 3 is purified Maspin. (D) Purified maspin-derivatives analyzed by SDS-PAGE followed by Coomassie blue staining. Lanes 1-4 are type Maspin,. Maspin(R330A), Maspin (ΔCT329), and Maspin(ΔCT315), respectively.

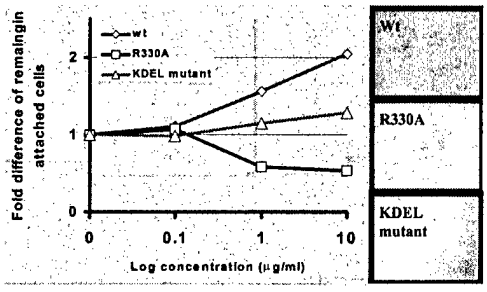


**Figure 4. The reactive site loop sequence of maspin is critical in maspin effect on cell detachment.** MDA-MB-435 cells were cultured in alpha medium supplemented with 5% FCS for 24 hours. The attached cells were then detached in a balanced salt solution depleted of divalent ion Ca++ for 30 minutes. The floating cells were removed. The cells remained attached were photographed (right panel) and counted using a Coulter Counter. The attached cells are normalized by the results of untreated control cells. Data represent the average of three repeats and the error bards stand for standard errors.

**Identification of the Molecular Targets of Maspin.**

To identify intracellular maspin-associated molecules, the full-length maspin cDNA fused in-frame with the LexA DNA-binding domain in a bait vector was used in yeast two-hybrid screening (15, 16). Two cDNA libraries, human prostate tumor cDNA library and HeLa cDNA library, were used to increase the statistical power of the screening as well as the probability to identify all maspin-interacting molecules. Out of $5x10^7$ diploid yeast cells, 28 clones (17 from the human prostate tumor library and 11 from HeLa library) showed specific interaction with the maspin bait and were subsequently sequenced. **Table 1** shows the results of the DNA sequence analyses using the NCBI BLAST search program. Three distinct types of proteins were identified as the potential maspin targets: Hsp90-α, Glutathione-S-transferase (μ3 and o) and histone deacetylase.

Table 1. Screening of Candidate Maspin Interactors by Yeast-two-hybrid System

| Candidate Maspin-interactors | Frequency of Identification | |
|---|---|---|
| | Primary Prostate Tumor Library | HeLa Library |
| HSP 90-1-alpha | 4 | 3 |
| GST M3 | 3 | 1 |
| GST Omega | 1 | 0 |
| Histone Deacetylase | 0 | 1 |

Figure 5A shows the subsequent confirmatory yeast-two-hybrid results using maspin bait and subcloned Hsp90 sequence. Independently, as shown in Figure 5B, Hsp90 in DU145 cell lysate was specifically pulled down by GST-maspin on glutathione affinity column. While the significance of maspin interaction with GST and histone deacetylase has to be further investigated, the identification of Hsp90 as a maspin-associated molecule is in good agreement with the evidence that maspin interacts with Hsp90 and RIP in TNF-α treated PC cells (**Figure 1**).

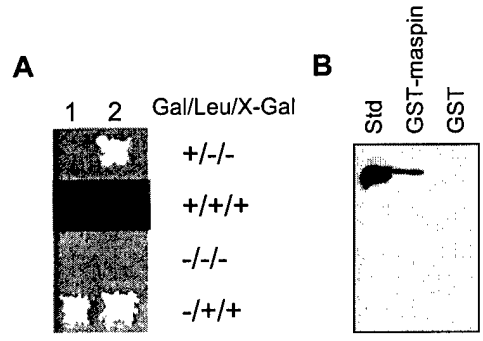


Figure 5. Hsp90 was identified as one of the maspin-associated molecules. (A): The confirmatory yeast-two-hybrid screenning using or randomly chosen bait (panel 1) or LexA-maspin bait (panel 2) to interact with subcloned Hsp90 cDNA prey. The specific interactions gave rise to galactose (Gal)-dependent and Leucine (Leu)-independent growth as well as positive (blue color) β–galactosidase activity in the presence of X-Gal substrate. (B): *In vitro* interaction between maspin and Hsp90 in GST-pull down assay. DU145 cell lysate was incubated with glutathione column preloaded with GST or GST-maspin fusion proteins. The subsequent glutathione eluents were analyzed by Hsp90 western blotting. Used as a positive control was commercially available purified Hsp90 (std).